

Low Rank Quaternion Matrix Recovery via Logarithmic Approximation

Liqiao Yang^a, Jifei Miao^a, Kit Ian Kou^{a,*}

^a*Department of Mathematics, Faculty of Science and Technology, University of Macau, Macau 999078, China*

Abstract

In color image processing, image completion aims to restore missing entries from the incomplete observation image. Recently, great progress has been made in achieving completion by approximately solving the rank minimization problem. In this paper, we utilize a novel quaternion matrix logarithmic norm to approximate rank under the quaternion matrix framework. From one side, unlike the traditional matrix completion method that handles RGB channels separately, the quaternion-based method is able to avoid destroying the structure of images via putting the color image in a pure quaternion matrix. From the other side, the logarithmic norm induces a more accurate rank surrogate. Based on the logarithmic norm, we take advantage of not only truncated technique but also factorization strategy to achieve image restoration. Both strategies are optimized based on the alternating minimization framework. The experimental results demonstrate that the use of logarithmic surrogates in the quaternion domain is more superior in solving the problem of color images completion.

Keywords: Image completion, low rank, quaternion matrix, logarithmic norm.

1. Introduction

Image completion is one of the key branches in image processing, which has attracted extensive research interests in recent years [1, 2, 3, 4]. When

*Corresponding author

Email addresses: liqiaoyoung@163.com (Liqiao Yang), jifmiao@163.com (Jifei Miao), kikou@umac.mo (Kit Ian Kou)

processing color images, the most traditional matrix-based image completion algorithms handle the three-dimensional data by unfolding it into matrices, which breaks the inherent correlation among RGB channels. It would cause some important information to be lost. This method of matrix-based image completion is devoted to solving the following model

$$\min_{\mathbf{X}} f(\mathbf{X}), \quad \text{s.t.} \quad P_{\Omega}(\mathbf{X} - \mathbf{M}) = 0, \quad (1)$$

where $f(\mathbf{X})$ is the cost function, $\mathbf{M} \in \mathbb{R}^{m \times n}$ is the observed matrix with missing entries, and $\mathbf{X} \in \mathbb{R}^{m \times n}$ is the recovered matrix. The linear operation $P_{\Omega}(\cdot)$ is developed to indicate the elements in Ω with 1 representing observed changeless elements and 0 representing missing elements. Since the structure of visual data has strong non-local self-similarity, it normally exhibits low rank characteristics [5]. Therefore, the cost function in (1) can be replaced by the rank function, and the low rank matrix completion (LRMC) model is formulated as

$$\min_{\mathbf{X}} \text{rank}(\mathbf{X}), \quad \text{s.t.} \quad P_{\Omega}(\mathbf{X} - \mathbf{M}) = 0. \quad (2)$$

As a combined optimization problem, problem (2) is generally solved by optimizing a convex proxy of the rank function [6], because directly dealing with the rank function is NP-hard. In the previous study [6], the nuclear norm of the matrix ($\|\mathbf{X}\|_* = \sum_{i=1}^{\min(m,n)} \sigma_i(\mathbf{X})$, where $\sigma_i(\mathbf{X})$ is the i th singular value of \mathbf{X}) is proved to be effective in replacing the rank function.

Many existing studies demonstrate that LRMC algorithms based on the nuclear norm may produce sub-optimal results because every singular value is processed equally [1, 7]. This approach goes against the fact that a larger singular value may contain more rich and useful information than a smaller one [1, 8]. To overcome these shortcomings, many nonconvex alternatives have been designed. For example, the truncated nuclear norm $\|\mathbf{X}\|_r = \sum_{i=r+1}^{\min(m,n)} \sigma_i(\mathbf{X})$ (TNN), the sum of $\min(m, n) - r$ minimum singular values of \mathbf{X} , is proposed in [1]. Moreover, the proposed two-step optimization process in [1] is effective. There are other similar surrogates to TNN, such as weighted nuclear norm [7] and weighted Schatten p-norm [8]. Similarly, the log-determinant alternate, *i.e.*, $L(\mathbf{X}, \epsilon) = \sum_{i=r+1}^{\min(m,n)} \log(\sigma_i(\mathbf{X}) + \epsilon)$ with $\epsilon > 0$, is also proved to be a more precise approximation of the rank than nuclear norm [9, 10]. The value of the logarithmic function becomes gentle as the singular values increase, meanwhile, the smaller singular values can be penalized more.

The strategies mentioned above are based on optimizing the approximation of the rank, which need to process whole singular value decomposition (SVD) of the matrix \mathbf{X} . Whereas, the computational complexity of SVD is high, which makes the promotion of high dimensional or big data have limitations [2, 11, 12]. To address this concern, the low rank matrix factorization (LRMF) is applied to matrix completion. These methods describe the low rank property of target matrix \mathbf{X} by factorizing it to two smaller factor matrices, *i.e.*, $\mathbf{X} = \mathbf{UV}^T$, where $\mathbf{U} \in \mathbb{R}^{m \times r}$ and $\mathbf{V} \in \mathbb{R}^{n \times r}$ with $r \ll \min(m, n)$. Although this method naturally satisfies the low rank requirement of the target matrix and also benefits from fast numerical optimization, it lacks the estimated value rank of \mathbf{X} in many situations. In [11], this problem is solved by an approximate skill. Besides, using a factorized approach instead of the spectral norm defined by one kind of weighted nuclear norm, would lead to a local minimum solution [13].

There is a necessary dimensional reduction operation based on LRMC to process color image completion. Because the above matrix-based approaches are focused on two dimensional data, color images can only be processed separately for RGB channels. In this way, they may lose the inner relationships among the three channels. In this regard, color image processing based on the quaternion framework has received widespread attention. Thanks to the structure of quaternion itself, each pixel of the color image can be represented by a pure quaternion to form a quaternion matrix. This representation is fully utilized in color images edge detection [14], color face recognition [15], color image denoising [16, 17], color image completion [3, 4], and so on.

In particular, when processing color image completion in the quaternion domain, the authors extended a low rank quaternion approximation (LRMA) model from LRMC [3]. It based on three nonconvex functions for approximating the rank of the quaternion matrix, including weighted Schatten p-norm, Laplace approximation, and Geman approximation. All these functions highlight the advantages of the quaternion matrix that have been verified experimentally and theoretically. However, as described above in the matrix cases, these approaches need to process fully quaternion singular value decomposition (QSVD) for quaternion matrix with expensive computational cost. To overcome this imperfection, the LRMF strategies are extended to the quaternion domain [4]. The authors factorized the target quaternion matrix to two-factor quaternion matrices and designed three quaternion-based bilinear factor matrix norm factorization methods for low-rank quaternion matrix completion (LRQMC). The methods of LRQMC include quaternion double

Frobenius norm (Q-DFN), quaternion double nuclear norm (Q-DNN), and quaternion Frobenius/nuclear norm (Q-FNN). All variables are optimized under the alternating direction method of multipliers (ADMM) framework which is similar to the real field. These factorized-based approaches only need to handle two smaller quaternion matrices. Thus considerable computational cost could be reduced.

In order to approximate the rank more accurately and effectively in the quaternion domain that takes full advantage of the color image structure, we develop two algorithms for LRQMC named Quaternion Logarithmic norm-based Factorization (QLNF) and Truncated Quaternion Logarithmic norm-based Approximation (TQLNA). Meanwhile, these two algorithms can narrow the gap between low-rank minimization and low-rank factorization. In this paper, a new quaternion logarithmic norm (QLN) is introduced as a non-convex replacement of rank, where the low rank can be more accurately depicted than traditional approximation methods like quaternion nuclear norm (QNN). Then, we adopt QLN to two smaller quaternion matrices, factor quaternion matrices of the target quaternion matrix in QLNF. In TQLNA, we truncate QLN and then optimize the target quaternion matrix directly by using the truncated quaternion logarithmic norm (TQLN). Concretely, the main contributions of this paper are summarized as follows:

- We propose a new nonconvex surrogate QLN for the rank of quaternion matrix with the guarantee of a surrogate theorem, and act QLN on factor quaternion matrix.
- The rank of the quaternion matrix would not be changed by the influence of the largest r singular values. So the proposed TQLN is operated by truncating the largest r singular values and then by adopting QLN in the truncated issue.
- For surrogate QLN, the fast iterative shrinkage thresholding algorithm (FISTA) is used to optimize the factor quaternion matrix. For TQLN, the ADMM based algorithm is used to efficiently solve the optimization problems. The experimental results prove that our method is effective in color image completion.

The rest of this paper is organized in the following structure. In Section 2, related notations and preliminary knowledge in the quaternion domain will be reviewed. In Section 3, we will discuss the quaternion-based model for

image completion and depict QLNf and TQLNA algorithms. In Section 4, this study will display the numerical experiment to compare other algorithms, and then a conclusion will be presented in Section 5. Part of the proofs will be listed in the Appendix.

2. Notations and preliminaries

In this section, the main notations and the preliminary knowledge based on quaternions adopted throughout this paper are introduced briefly.

2.1. Notations

we use a , \mathbf{a} , and \mathbf{A} to denote scalar, vector and matrix in real domain \mathbb{R} , respectively. A dot above the variables (\dot{a} , $\dot{\mathbf{a}}$, and $\dot{\mathbf{A}}$) are to denote the variables (scalars, vectors, and matrices) in the quaternion domain \mathbb{H} . Besides, the complex space is denoted by \mathbb{C} . Both $\mathbf{I}_{r \times r}$ and \mathbf{I}_r represent the $r \times r$ identity matrix. $\Re(\dot{a})$ is the real part of quaternion \dot{a} . $(\cdot)^T$, $(\cdot)^*$, $(\cdot)^H$ and $(\cdot)^{-1}$ represent the transpose, conjugate, conjugate transpose and the inverse of \cdot , respectively. $|\cdot|$, $\|\cdot\|_F$, $\|\cdot\|_*$ are the absolute value of modulus, Frobenius norm, and nuclear norm of \cdot , respectively. The inner product of \circ_1 and \circ_2 is defined as $\langle \circ_1 \cdot \circ_2 \rangle \triangleq \text{tr}(\circ_1^H \circ_2)$, and $\text{tr}(\cdot)$ is the trace function.

2.2. Preliminary sketch of quaternion-based knowledge

Quaternion space \mathbb{H} was first proposed by W. Hamilton [18]. As a generalization of complex number, a quaternion number $\dot{a} \in \mathbb{H}$ can be represented by Cartesian form

$$\dot{a} = a_0 + a_1i + a_2j + a_3k, \quad (3)$$

where $a_l \in \mathbb{R}(l = 0, 1, 2, 3)$, and i, j, k are three imaginary number units which have the following relationships

$$\begin{cases} i^2 = j^2 = k^2 = ijk = -1 \\ ij = -ji = k, jk = -kj = i, ki = -ik = j. \end{cases} \quad (4)$$

$\Re(\dot{a}) \triangleq a_0$ is the real part of \dot{a} . $\Im(\dot{a}) \triangleq a_1i + a_2j + a_3k$ is the imaginary part of \dot{a} . Hence $\dot{a} = \Re(\dot{a}) + \Im(\dot{a})$. Besides, when real part $a_0 = 0$, \dot{a} is a pure quaternion. The conjugate and the modulus of \dot{a} are defined as: $\dot{a}^* = a_0 - a_1i - a_2j - a_3k$ and $|\dot{a}| = \sqrt{\dot{a}\dot{a}^*} = \sqrt{a_0^2 + a_1^2 + a_2^2 + a_3^2}$, separately.

Assuming two quaternions \dot{a} and $\dot{b} \in \mathbb{H}$, the addition and multiplication are separately defined as following

$$\dot{a} + \dot{b} = (a_0 + b_0) + (a_1 + b_1)i + (a_2 + b_2)j + (a_3 + b_3)k$$

$$\begin{aligned} \dot{a}\dot{b} &= (a_0b_0 - a_1b_1 - a_2b_2 - a_3b_3) \\ &\quad + (a_0b_1 + a_1b_0 + a_2b_3 - a_3b_2)i \\ &\quad + (a_0b_2 - a_1b_3 + a_2b_0 + a_3b_1)j \\ &\quad + (a_0b_3 + a_1b_2 - a_2b_1 + a_3b_0)k. \end{aligned}$$

What calls for special attention is that the multiplication in the quaternion domain is not commutative $\dot{a}\dot{b} \neq \dot{b}\dot{a}$.

The quaternion matrix $\dot{\mathbf{A}} = (\dot{a}_{ij}) \in \mathbb{H}^{M \times N}$, where $\dot{\mathbf{A}} = \mathbf{A}_0 + \mathbf{A}_1i + \mathbf{A}_2j + \mathbf{A}_3k$. In the definition of $\dot{\mathbf{A}}$, $\mathbf{A}_l \in \mathbb{R}^{M \times N}$ ($l = 0, 1, 2, 3$) which are real matrices. When $\mathbf{A}_0 = \mathbf{0}$, $\dot{\mathbf{A}}$ is a pure quaternion matrix. The Forbenius norm is defined as: $\|\dot{\mathbf{A}}\|_F = \sqrt{\sum_{i=1}^M \sum_{j=1}^N |\dot{a}_{ij}|^2} = \sqrt{\text{tr}(\dot{\mathbf{A}}^H \dot{\mathbf{A}})}$. The form using Cayley-Dickson notation [19] is $\dot{\mathbf{A}} = \mathbf{A}_p + \mathbf{A}_qj$, where \mathbf{A}_p and $\mathbf{A}_q \in \mathbb{C}^{M \times N}$ are complex matrices. Hence, the representation of quaternion matrix $\dot{\mathbf{A}}$ can be denoted as an isomorphic complex matrix $\mathbf{A}_c \in \mathbb{C}^{2M \times 2N}$

$$\mathbf{A}_c = \begin{pmatrix} \mathbf{A}_p & \mathbf{A}_q \\ -\mathbf{A}_q^* & \mathbf{A}_p^* \end{pmatrix}_{2M \times 2N}, \quad (5)$$

where $\mathbf{A}_p = \mathbf{A}_0 + \mathbf{A}_1i \in \mathbb{C}^{M \times N}$ and $\mathbf{A}_q = \mathbf{A}_2 + \mathbf{A}_3i \in \mathbb{C}^{M \times N}$.

Definition 1. (*The rank of quaternion matrix [20]*): For a quaternion matrix $\dot{\mathbf{A}} = (\dot{a}_{ij}) \in \mathbb{H}^{M \times N}$, the maximum number of right (left) linearly independent columns (rows) is defined as the rank of $\dot{\mathbf{A}}$.

Theorem 1. (*QSVD [20]*): Given a quaternion matrix $\dot{\mathbf{A}} \in \mathbb{H}^{M \times N}$ be of rank r . There are two unitary quaternion matrices $\dot{\mathbf{U}} \in \mathbb{H}^{M \times M}$ and $\dot{\mathbf{V}} \in \mathbb{H}^{N \times N}$ such that

$$\dot{\mathbf{A}} = \dot{\mathbf{U}} \begin{pmatrix} \Sigma_r & \mathbf{0} \\ \mathbf{0} & \mathbf{0} \end{pmatrix} \dot{\mathbf{V}}^H = \dot{\mathbf{U}} \Lambda \dot{\mathbf{V}}^H, \quad (6)$$

where $\Sigma_r = \text{diag}(\sigma_1, \dots, \sigma_r) \in \mathbb{R}^{r \times r}$, and all singular values $\sigma_i > 0, i = 1, \dots, r$.

The connection of the QSVD of $\dot{\mathbf{A}}$ and the SVD of the isomorphic complex matrix $\mathbf{A}_c \in \mathbb{C}^{2M \times 2N}$ ($\mathbf{A}_c = \mathbf{U}\dot{\mathbf{A}}\mathbf{V}^H$) is listed as follows [21]

$$\begin{cases} \dot{\mathbf{\Lambda}} = \text{row}_{\text{odd}}(\text{col}_{\text{odd}}(\dot{\mathbf{A}})), \\ \dot{\mathbf{U}} = \text{col}_{\text{odd}}(\mathbf{U}_1) + \text{col}_{\text{odd}}(-(\mathbf{U}_2)^*)j, \\ \dot{\mathbf{V}} = \text{col}_{\text{odd}}(\mathbf{V}_1) + \text{col}_{\text{odd}}(-(\mathbf{V}_2)^*)j, \end{cases} \quad (7)$$

then we have $\dot{\mathbf{A}} = \dot{\mathbf{U}}\dot{\mathbf{\Lambda}}\dot{\mathbf{V}}^H$, where $\mathbf{U} = \begin{pmatrix} \mathbf{U}_1)_{M \times 2M} \\ (\mathbf{U}_2)_{M \times 2M} \end{pmatrix}$ and $\mathbf{V} = \begin{pmatrix} \mathbf{V}_1)_{N \times 2N} \\ (\mathbf{V}_2)_{N \times 2N} \end{pmatrix}$. The odd rows and odd columns of \star are represented by $\text{row}_{\text{odd}}(\star)$ and $\text{col}_{\text{odd}}(\star)$ respectively.

Utilizing the above property and theorem, the QSVD can be obtained by computing the classical SVD of the complex matrix \mathbf{A}_c . Moreover, we can see that the number of positive singular values r is the rank of $\dot{\mathbf{A}}$ [20]. For a more detailed introduction of quaternion algebra, please refer to [20, 22]. Following the Theorem 1, we can get the definition of quaternion matrix nuclear norm (QNN).

Definition 2. (QNN) [3, 16]: Given $\dot{\mathbf{A}} \in \mathbb{H}^{M \times N}$, the nuclear norm of the quaternion matrix is $\|\dot{\mathbf{A}}\|_* = \sum_{i=1}^{\min(M,N)} \sigma_i(\dot{\mathbf{A}})$, where σ_i can be obtained by the QSVD of $\dot{\mathbf{A}}$.

Theorem 2. (Binary factorization framework [4]): For any quaternion matrix $\dot{\mathbf{X}} \in \mathbb{H}^{M \times N}$ with $\text{rank}(\dot{\mathbf{X}}) = r \leq d$. Then the binary factorization framework is devised as

$$\dot{\mathbf{X}} = \dot{\mathbf{U}}\dot{\mathbf{V}}^H, \quad (8)$$

where $\dot{\mathbf{U}} \in \mathbb{H}^{M \times d}$ and $\dot{\mathbf{V}} \in \mathbb{H}^{N \times d}$ such that $\text{rank}(\dot{\mathbf{U}}) = \text{rank}(\dot{\mathbf{V}}) = r$.

Definition 3. (Q-DFN [4]): Based on theorem 2, the quaternion double Frobenius norm is defined as

$$\|\dot{\mathbf{X}}\|_{Q\text{-DFN}} := \min_{\dot{\mathbf{U}}, \dot{\mathbf{V}}} \frac{1}{2} \|\dot{\mathbf{U}}\|_F^2 + \frac{1}{2} \|\dot{\mathbf{V}}\|_F^2. \quad (9)$$

$$\dot{\mathbf{X}} = \dot{\mathbf{U}}\dot{\mathbf{V}}^H$$

Essentially, whether it is based on matrix or quaternion matrix, the double Frobenius norm is the nuclear norm [2, 4, 23], i.e., $\|\dot{\mathbf{X}}\|_{Q\text{-DFN}} = \|\dot{\mathbf{X}}\|_*$.

3. Quaternion-based model for image completion

In this section, we first review the quaternion-based completion related works, and then introduce our quaternion-based low rank completion strategies.

3.1. Related work and low rank quaternion matrix completion

In the related optimized field of completion, a new surrogate, logarithmic norm was devised [24], and was utilized in factorized framework to get the recovery. The logarithmic norm of the given matrix $\mathbf{X} \in \mathbb{R}^{M \times N}$ is defined as

$$\|\mathbf{X}\|_L^p = \sum_{i=1}^{\min(M,N)} \log(\sigma_i^p(\mathbf{X}) + \epsilon), \quad (10)$$

where σ_i can be obtained by computing SVD of \mathbf{X} . The main advantage of using the logarithmic norm is that it has a superior sparse substitution of rank over the convex envelope of the nuclear norm [24, 25]. For example, when $\mathbf{X} = x \in \mathbb{R}$, $\text{rank}(x) = 0$ if $x = 0$ and $\text{rank}(x) = 1$, otherwise. Supposing $|x| \leq M$, $\frac{\|x\|_*}{M} = \frac{|x|}{M}$ is the convex envelop of $\text{rank}(x) = 0$ on $\{x \mid |x| \leq M\}$ [25, 26]. The intuitive explanation behind the idea of using logarithmic function to approximate rank can be found in Figure 1. When ϵ is a small positive constant, logarithmic norm would be closer to $\text{rank}(x)$ than the convex envelop [24].

The classic LRMC model that fundamentally optimizes two-dimensional data like grayscale images completion is briefly introduced in (2). Therefore, when processing color images, the model in (2) needs to disassemble RGB channels, while LRQMC model can assemble RGB channels. As an extended model from LRMC, the model of LRQMC can be represented as [3]

$$\min_{\dot{\mathbf{X}}} \text{rank}(\dot{\mathbf{X}}), \quad \text{s.t.} \quad P_{\Omega}(\dot{\mathbf{X}} - \dot{\mathbf{M}}) = 0, \quad (11)$$

where $\dot{\mathbf{M}}$ is the given partial observed quaternion matrix (missing color image). $\dot{\mathbf{X}} \in \mathbb{H}^{M \times N}$ is the recovery quaternion matrix (recovered color image). The linear operation $P_{\Omega}(\cdot)$ indicating the elements in Ω are presented as 1 for the observed changeless entries and 0 for missing entries.

The main completion models in the quaternion domain can be divided into two lines: low rank minimization and low rank factorization. Similar to LRMC, the rank function is hard to be optimized in model (11). Hence, for

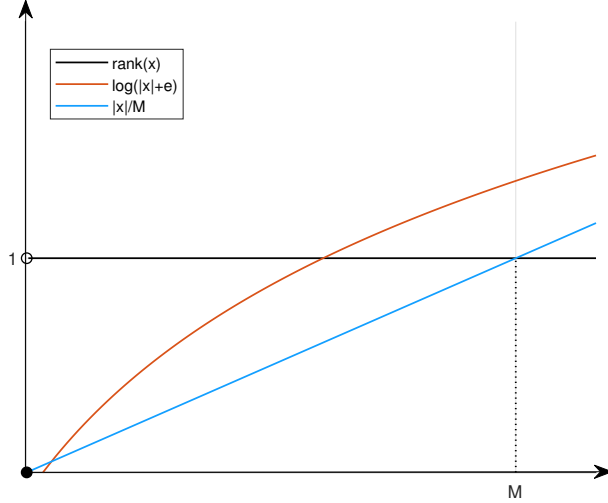


Figure 1: The rank, the convex envelop of rank (nuclear norm), and the logarithmic norm for scalar x

the first line, based on Definition 2, the model of low rank minimization can be written as

$$\min_{\dot{\mathbf{X}}} \|\dot{\mathbf{X}}\|_*, \quad \text{s.t.} \quad P_{\Omega}(\dot{\mathbf{X}} - \dot{\mathbf{M}}) = 0. \quad (12)$$

Almost all optimizations based on (12) are aiming to improve QNN, like a more general Schattern p -norm ($\|\dot{\mathbf{X}}\|_{Q-S_p} = (\sum_{i=1}^{\min(M,N)} \sigma_i^p(\dot{\mathbf{X}}))^{\frac{1}{p}}, 0 < p < \infty$) [3, 16], and a Log-determinant norm ($L(\dot{\mathbf{X}}, \epsilon) = \sum_{i=r+1}^{\min(m,n)} \log(\sigma_i(\dot{\mathbf{X}}) + \epsilon)$ with $\epsilon > 0$) [3]. When we let $p = 1$, the Schattern p -norm is the frequently used nuclear norm. The mentioned methods have proved their effectiveness theoretically and experimentally in processing color image completion.

In addition to the methods listed above, the low rank factorization has been also found to be an important line for completion. Based on the Theorem 2 and Definition 3, the model of low rank factorization can be written as [4]

$$\min_{\dot{\mathbf{X}}} \|\dot{\mathbf{X}}\|_{Q-DFN}, \quad \text{s.t.} \quad P_{\Omega}(\dot{\mathbf{X}} - \dot{\mathbf{M}}) = 0. \quad (13)$$

After inducing a nonnegative parameter λ to balance the loss function and

the low rank regularization, (13) can be further represented as

$$\begin{aligned} \min_{\dot{\mathbf{U}}, \dot{\mathbf{V}}, \dot{\mathbf{X}}} \frac{\lambda}{2} (\|\dot{\mathbf{U}}\|_F^2 + \|\dot{\mathbf{V}}\|_F^2) + \frac{1}{2} \|P_\Omega(\dot{\mathbf{X}} - \dot{\mathbf{M}})\|_F \\ \text{s.t. } \dot{\mathbf{X}} = \dot{\mathbf{U}}\dot{\mathbf{V}}^H. \end{aligned} \quad (14)$$

In this way, the goal is shifted from calculating the entire QSVD of large-scale $\dot{\mathbf{X}}$ to optimizing bi-factor quaternion matrices that have smaller dimensions.

3.2. The proposed Quaternion-based Logarithmic Norm Factorization (QLNF)

As described above, because of the geometric structure of the quaternion itself, the processing of color images in the quaternion domain can maintain the connection between channels as much as possible. In this section, enlightened by the definition of the logarithmic norm in [24], we define the quaternion-based logarithmic norm. Then, we establish the equivalence relation between quaternion-based Logarithmic norm and bi-factor quaternion matrix factorization. Eventually, the optimization process is given.

Definition 4. (QLN): Given $\dot{\mathbf{X}} \in \mathbb{H}^{M \times N}$, the logarithmic norm of the quaternion matrix with $0 \leq p \leq 1$ and $\epsilon > 0$ is

$$\|\dot{\mathbf{X}}\|_L^p = \sum_{i=1}^{\min(M,N)} \log(\sigma_i^p(\dot{\mathbf{X}}) + \epsilon), \quad (15)$$

where σ_i can be obtained by the QSVD of $\dot{\mathbf{X}}$.

The rank is a real number, which is analogous to the situation in the real domain. Learning from Figure 1, the QLN is a more precise approximation than QNN. Moreover, inspired by the bi-factor surrogate theorem for matrix logarithmic norm in [24], and Theorem 2, we establish the bi-factor surrogate theorem for QLN.

Theorem 3. : For any quaternion matrix $\dot{\mathbf{X}} \in \mathbb{H}^{M \times N}$ with $\text{rank}(\dot{\mathbf{X}}) = r \leq d \leq \{M, N\}$. There exist $\dot{\mathbf{U}} \in \mathbb{H}^{M \times d}$ and $\dot{\mathbf{V}} \in \mathbb{H}^{N \times d}$ such that $\dot{\mathbf{X}} = \dot{\mathbf{U}}\dot{\mathbf{V}}^H$. Then we have

$$\|\dot{\mathbf{X}}\|_L^{1/2} := \min_{\substack{\dot{\mathbf{U}}, \dot{\mathbf{V}} \\ \dot{\mathbf{X}} = \dot{\mathbf{U}}\dot{\mathbf{V}}^H}} \frac{1}{2} \|\dot{\mathbf{U}}\|_L + \frac{1}{2} \|\dot{\mathbf{V}}\|_L. \quad (16)$$

The proof of Theorem 3 can be found in the Appendix.

Based on Definition 4 and Theorem 3, we present the following completion model with the quaternion-based framework

$$\min_{\dot{\mathbf{X}}} \|\dot{\mathbf{X}}\|_L^{1/2}, \quad \text{s.t.} \quad P_\Omega(\dot{\mathbf{X}} - \dot{\mathbf{M}}) = 0, \quad (17)$$

Integrating the above questions into one formula, (17) can be further written as

$$\min_{\dot{\mathbf{U}}, \dot{\mathbf{V}}, \dot{\mathbf{X}}} \frac{\lambda}{2} (\|\dot{\mathbf{U}}\|_L^1 + \|\dot{\mathbf{V}}\|_L^1) + \|\mathbf{W} \odot (\dot{\mathbf{U}}\dot{\mathbf{V}}^H - \dot{\mathbf{M}})\|_F^2, \quad (18)$$

where $\mathbf{W} \in \mathbb{R}^{M \times N}$ denotes the location of the existing and missing entries, indicating by 1 and 0. \odot is the Hadamard product. When the multiplication is acted on the real matrix \mathbf{W} and the quaternion matrix $(\dot{\mathbf{U}}\dot{\mathbf{V}}^H - \dot{\mathbf{M}}) \in \mathbb{Q}^{M \times N}$, \odot still means element-wise multiplication. λ is a nonnegative parameter.

As in matrix-based situation, this model is full of challenges to be optimized. Inspired by the FISTA designed in the real domain [27], we induce the FISTA to update under the alternating minimization framework. It means that at each iteration, we update factors in turn with other factors fixed. Assuming $\dot{\mathbf{U}}_{k+1}$ and $\dot{\mathbf{V}}_{k+1}$ is the updating results in the k th iteration. Specific steps are listed as follows

Updating $\dot{\mathbf{U}}$:

$$\dot{\mathbf{U}}_{k+1} = \arg \min_{\dot{\mathbf{U}}} \frac{\lambda}{2} \|\dot{\mathbf{U}}\|_L^1 + \|\mathbf{W} \odot (\dot{\mathbf{U}}\dot{\mathbf{V}}_k^H - \dot{\mathbf{M}})\|_F^2. \quad (19)$$

Let $\mathcal{Q}(\dot{\mathbf{U}}) = \|\mathbf{W} \odot (\dot{\mathbf{U}}\dot{\mathbf{V}}_k^H - \dot{\mathbf{M}})\|_F^2$. Analogous to the ADMM framework used in the complex and the quaternion domain [4, 28] and based on FISTA, the updating of $\dot{\mathbf{U}}_{k+1}$ can be written as:

$$\begin{cases} \hat{\mathbf{U}}_k = \dot{\mathbf{U}}_k + \omega_k(\dot{\mathbf{U}}_k - \dot{\mathbf{U}}_{k-1}) \\ \dot{\mathbf{U}}_{k+1} = \arg \min_{\dot{\mathbf{U}}} \Re(\langle \nabla \mathcal{Q}(\hat{\mathbf{U}}_k), \dot{\mathbf{U}} - \hat{\mathbf{U}}_k \rangle) + \frac{\mu_k}{2} \|\dot{\mathbf{U}} - \hat{\mathbf{U}}_k\|_F^2 + \frac{\lambda}{2} \|\dot{\mathbf{U}}\|_L^1, \end{cases} \quad (20)$$

where $t_k = \frac{1 + \sqrt{1 + 4t_{k-1}^2}}{2}$ and $\omega_k = \frac{t_{k-1}-1}{t_k}$. Further, we can get

$$\begin{cases} \hat{\mathbf{U}}_k = \dot{\mathbf{U}}_k + \omega_k(\dot{\mathbf{U}}_k - \dot{\mathbf{U}}_{k-1}). \\ \dot{\mathbf{U}}_{k+1} = \arg \min_{\dot{\mathbf{U}}} \frac{\lambda}{2} \|\dot{\mathbf{U}}\|_L^1 + \frac{\mu_k}{2} \|\dot{\mathbf{U}} - \hat{\mathbf{U}}_k + \frac{1}{\mu_k} \nabla \mathcal{Q}(\hat{\mathbf{U}}_k)\|_F^2 \end{cases} \quad (21)$$

It should be noted that the left and right generalized HR (GHR) of the real functions $\mathcal{Q}(\dot{\mathbf{U}})$ with quaternion variables are the same [29]. Consequently, according to the derivation theories for quaternion matrix in [29], the gradient of $\mathcal{Q}(\dot{\mathbf{U}})$ is computed as following

$$\begin{aligned}
\frac{\partial \mathcal{Q}(\dot{\mathbf{U}})}{\partial \dot{\mathbf{U}}^*} &= \frac{\partial Tr\{(\mathbf{W} \odot (\dot{\mathbf{U}}\dot{\mathbf{V}}_k^H - \dot{\mathbf{M}}))^H(\mathbf{W} \odot (\dot{\mathbf{U}}\dot{\mathbf{V}}_k^H - \dot{\mathbf{M}}))\}}{\partial \dot{\mathbf{U}}^*} \\
&= \mathbf{W} \odot (\Re(\dot{\mathbf{U}}\dot{\mathbf{V}}_k^H)\dot{\mathbf{V}}_k - \frac{1}{2}(\dot{\mathbf{V}}_k\dot{\mathbf{U}}^{*H})^T\dot{\mathbf{V}}_k - \Re(\dot{\mathbf{M}})\dot{\mathbf{V}}_k + \frac{1}{2}\dot{\mathbf{M}}^*\dot{\mathbf{V}}_k) \\
&= \mathbf{W} \odot (\frac{1}{2}\dot{\mathbf{U}}\dot{\mathbf{V}}_k^H\dot{\mathbf{V}}_k - \frac{1}{2}\dot{\mathbf{M}}\dot{\mathbf{V}}_k).
\end{aligned} \tag{22}$$

Then, (21) can be rewritten as

$$\begin{cases} \hat{\mathbf{U}}_k = \dot{\mathbf{U}}_k + \omega_k(\dot{\mathbf{U}}_k - \dot{\mathbf{U}}_{k-1}). \\ \hat{\mathbf{U}}_{k+1} = \arg \min_{\dot{\mathbf{U}}} \frac{\lambda}{2} \|\dot{\mathbf{U}}\|_L^1 + \frac{\mu_k}{2} \|\dot{\mathbf{U}} - \hat{\mathbf{U}}_k + \frac{1}{2\mu_k}\mathbf{W} \odot (\hat{\mathbf{U}}_k\dot{\mathbf{V}}_k^H - \dot{\mathbf{M}})\dot{\mathbf{V}}_k\|_F^2 \end{cases} \tag{23}$$

The next problem is how to obtain the optimal of (23). To solve this problem, we establish the following theorem to get an approximate expression.

Theorem 4. (Quaternion logarithmic singular value thresholding (QLSVT)) : For any quaternion matrix $\lambda > 0$ and $\dot{\mathbf{Y}} \in \mathbb{H}^{M \times N}$, the QSVD of $\dot{\mathbf{Y}}$ is $\dot{\mathbf{Y}} = \dot{\mathbf{U}}_{\dot{\mathbf{Y}}}(\Lambda_{\dot{\mathbf{Y}}})\dot{\mathbf{V}}_{\dot{\mathbf{Y}}}^H$. Then the closed solution of the problem

$$\arg \min_{\dot{\mathbf{X}}} \frac{1}{2} \|\dot{\mathbf{Y}} - \dot{\mathbf{X}}\|_F^2 + \lambda \|\dot{\mathbf{X}}\|_L^1 \tag{24}$$

is provided by $\dot{\mathbf{X}} = \dot{\mathbf{U}}_{\dot{\mathbf{Y}}}\mathcal{L}_{\lambda,\epsilon}(\Lambda_{\dot{\mathbf{Y}}})\dot{\mathbf{V}}_{\dot{\mathbf{Y}}}^H$. Because $\Lambda_{\dot{\mathbf{Y}}}$ consists of real numbers, the form of $\mathcal{L}_{\lambda,\epsilon}(\cdot)$ is similar to the real case [24]. The soft thresholding operator $\mathcal{L}_{\lambda,\epsilon}(\cdot)$ is defined as

$$\mathcal{L}_{\lambda,\epsilon}(x) := \begin{cases} 0, & \Delta \leq 0 \\ \arg \min_{a \in \{0, \frac{1}{2}(x-\epsilon+\sqrt{\Delta})\}} h(a), & \Delta > 0 \end{cases} \tag{25}$$

where $\Delta = (x - \epsilon)^2 - 4(\lambda - x\epsilon)$ and function $h(a) := \frac{1}{2}(a - x)^2 + \lambda \log(a + \epsilon)$ is $\mathbb{R}^+ \rightarrow \mathbb{R}^+$.

Proof: For quaternion matrices $\dot{\mathbf{X}} \in \mathbb{H}^{M \times N}$ and $\dot{\mathbf{Y}} \in \mathbb{H}^{M \times N}$, the QSVD of them is $\dot{\mathbf{X}} = \dot{\mathbf{U}}_{\dot{\mathbf{X}}}(\Lambda_{\dot{\mathbf{X}}})\dot{\mathbf{V}}_{\dot{\mathbf{X}}}^H$ and $\dot{\mathbf{Y}} = \dot{\mathbf{U}}_{\dot{\mathbf{Y}}}(\Lambda_{\dot{\mathbf{Y}}})\dot{\mathbf{V}}_{\dot{\mathbf{Y}}}^H$. Then we have

$$\begin{aligned}
& \frac{1}{2} \|\dot{\mathbf{Y}} - \dot{\mathbf{X}}\|_F^2 + \lambda \|\dot{\mathbf{X}}\|_L^1 \\
&= \frac{1}{2} (Tr(\dot{\mathbf{Y}}^H \dot{\mathbf{Y}}) - 2Tr(\dot{\mathbf{Y}}^H \dot{\mathbf{X}}) + Tr(\dot{\mathbf{X}}^H \dot{\mathbf{X}})) + \lambda \|\dot{\mathbf{X}}\|_L^1 \\
&= \frac{1}{2} (\sum_i \sigma_i(\dot{\mathbf{Y}}) - 2Tr(\dot{\mathbf{Y}}^H \dot{\mathbf{X}}) + \sum_i \sigma_i(\dot{\mathbf{X}})) + \lambda \|\dot{\mathbf{X}}\|_L^1 \\
&\geq \frac{1}{2} (\sum_i \sigma_i(\dot{\mathbf{Y}}) - 2\sigma_i(\dot{\mathbf{Y}}\sigma_i(\dot{\mathbf{X}}) + \sum_i \sigma_i(\dot{\mathbf{X}})) + \lambda \|\dot{\mathbf{X}}\|_L^1 \\
&= \sum_i \frac{1}{2} (\sigma_i(\dot{\mathbf{Y}}) - \sigma_i(\dot{\mathbf{X}}))^2 + \lambda \log(\sigma_i(\dot{\mathbf{X}}) + \epsilon),
\end{aligned} \tag{26}$$

where the first inequality follows from [30]. Based on the von Neumann's trace inequality in [30], $Tr(\dot{\mathbf{Y}}^H \dot{\mathbf{X}})$ reaches its upper bound $\sum_i \sigma_i(\dot{\mathbf{Y}})\sigma_i(\dot{\mathbf{X}})$ when $\dot{\mathbf{U}}_{\dot{\mathbf{X}}} = \dot{\mathbf{U}}_{\dot{\mathbf{Y}}}$, $\dot{\mathbf{V}}_{\dot{\mathbf{X}}} = \dot{\mathbf{V}}_{\dot{\mathbf{Y}}}$. Then we have

$$\begin{aligned}
& \min_{\dot{\mathbf{X}}} \frac{1}{2} \|\dot{\mathbf{Y}} - \dot{\mathbf{X}}\|_F^2 + \lambda \|\dot{\mathbf{X}}\|_L^1 \Leftrightarrow \\
& \min_{\{\sigma_i(\dot{\mathbf{X}}) \geq 0\}} \sum_i \frac{1}{2} (\sigma_i(\dot{\mathbf{Y}}) - \sigma_i(\dot{\mathbf{X}}))^2 + \lambda \log(\sigma_i(\dot{\mathbf{X}}) + \epsilon), \\
& \text{s.t. } \sigma_1(\dot{\mathbf{X}}) \geq \sigma_2(\dot{\mathbf{X}}) \geq \dots \geq \sigma_{\min\{M,N\}}(\dot{\mathbf{X}}) \geq 0.
\end{aligned} \tag{27}$$

Next, we study how to find the lower bound of optimal $\dot{\mathbf{X}}$. The singular value $\sigma_i(\dot{\mathbf{X}})$ can be determined by

$$\min_{\{\sigma_i(\dot{\mathbf{X}}) \geq 0\}} h(\sigma_i(\dot{\mathbf{X}})) = \frac{1}{2} (\sigma_i(\dot{\mathbf{Y}}) - \sigma_i(\dot{\mathbf{X}}))^2 + \lambda \log(\sigma_i(\dot{\mathbf{X}}) + \epsilon), \tag{28}$$

which is differentiable in $[0, +\infty)$. Hence, we can get the first-order derivative of $h(\sigma_i(\dot{\mathbf{X}}))$

$$h'(\sigma_i(\dot{\mathbf{X}})) = \sigma_i(\dot{\mathbf{X}}) - \sigma_i(\dot{\mathbf{Y}}) + \frac{\lambda}{\sigma_i(\dot{\mathbf{X}}) + \epsilon}, \tag{29}$$

further, we have

$$(\sigma_i(\dot{\mathbf{X}}) + \epsilon)h'(\sigma_i(\dot{\mathbf{X}})) = \sigma_i^2(\dot{\mathbf{X}}) - (\sigma_i(\dot{\mathbf{Y}}) - \epsilon)\sigma_i(\dot{\mathbf{X}}) + \lambda - \sigma_i(\dot{\mathbf{Y}})\epsilon, \tag{30}$$

where the $\Delta_i = (\sigma_i(\dot{\mathbf{Y}}) - \epsilon)^2 - 4(\lambda - \sigma_i(\dot{\mathbf{Y}})\epsilon)$. For (30), if $\Delta_i \leq 0$, the LHS $(\sigma_i(\dot{\mathbf{X}}) + \epsilon)h'(\sigma_i(\dot{\mathbf{X}})) \geq 0$. It means that $h(\sigma_i(\dot{\mathbf{X}}))$ is monotonically increasing, so 0 is the optimal solution. If $\Delta_i > 0$, $h'(\sigma_i(\dot{\mathbf{X}})) = 0$ in two roots. Based on the possible monotony of the function $h(\sigma_i(\dot{\mathbf{X}}))$, the results only include 0 root and the larger root $\frac{1}{2}(\sigma_i(\dot{\mathbf{Y}}) - \epsilon + \sqrt{\Delta - i})$, which is shown in (25). \blacksquare

Based on the above discussion, the QLSVT can be applied to (23) for updating $\dot{\mathbf{U}}$. By similar approach, we can get the update of $\dot{\mathbf{V}}$.

Updating $\dot{\mathbf{V}}$:

$$\dot{\mathbf{V}}_{k+1} = \arg \min_{\dot{\mathbf{V}}} \frac{\lambda}{2} \|\dot{\mathbf{V}}\|_L^1 + \|\mathbf{W} \odot (\dot{\mathbf{U}}_{k+1} \dot{\mathbf{V}}^H - \dot{\mathbf{M}})\|_F^2. \quad (31)$$

Let $\mathcal{P}(\dot{\mathbf{V}}) = \|\mathbf{W} \odot (\dot{\mathbf{U}}_{k+1} \dot{\mathbf{V}}^H - \dot{\mathbf{M}})\|_F^2$. Based on the FISTA, the update of $\dot{\mathbf{V}}_{k+1}$ can be written as

$$\begin{cases} \hat{\dot{\mathbf{V}}}_k = \dot{\mathbf{V}}_k + \omega_k(\dot{\mathbf{V}}_k - \dot{\mathbf{V}}_{k-1}). \\ \dot{\mathbf{V}}_{k+1} = \arg \min_{\dot{\mathbf{V}}} \frac{\lambda}{2} \|\dot{\mathbf{V}}\|_L^1 + \frac{\mu_k}{2} \|\dot{\mathbf{V}} - \hat{\dot{\mathbf{V}}}_k + \frac{1}{\mu_k} \nabla \mathcal{P}(\hat{\dot{\mathbf{V}}}_k)\|_F^2. \end{cases} \quad (32)$$

Using the theories of quaternion matrix derivatives, the gradient of $\mathcal{P}(\hat{\dot{\mathbf{V}}})$ is

$$\frac{\partial \mathcal{P}(\hat{\dot{\mathbf{V}}})}{\partial \hat{\dot{\mathbf{V}}}^*} = \mathbf{W} \odot \left(\frac{1}{2} \hat{\dot{\mathbf{V}}} \dot{\mathbf{U}}_{k+1}^H \dot{\mathbf{U}}_{k+1} - \frac{1}{2} \dot{\mathbf{M}}^H \dot{\mathbf{U}}_{k+1} \right). \quad (33)$$

Taking the above gradient into (32), we can get

$$\begin{cases} \hat{\dot{\mathbf{V}}}_k = \dot{\mathbf{V}}_k + \omega_k(\dot{\mathbf{V}}_k - \dot{\mathbf{V}}_{k-1}). \\ \dot{\mathbf{V}}_{k+1} = \arg \min_{\dot{\mathbf{V}}} \frac{\lambda}{2} \|\dot{\mathbf{V}}\|_L^1 + \frac{\mu_k}{2} \|\dot{\mathbf{V}} - \hat{\dot{\mathbf{V}}}_k + \frac{1}{2\mu_k} \mathbf{W} \odot (\hat{\dot{\mathbf{V}}}_k \dot{\mathbf{U}}_{k+1}^H - \dot{\mathbf{M}}^H) \hat{\dot{\mathbf{U}}}_{k+1}\|_F^2. \end{cases} \quad (34)$$

Then the QLSVT can be used to solve the above model. The whole steps of the QLN algorithm are given in Algorithm 1.

3.3. The proposed Truncated Quaternion-based Logarithmic Norm Approximation (TQLNA)

As we mentioned in the problem of matrix low rank optimization above, the truncated nuclear norm can achieve a better approximation of the rank function than the nuclear norm by using a two-step iterative scheme [1]. Motivated by this approach, we incorporate the truncated skill and QLN to induce the truncated quaternion-based logarithmic norm as follows

Algorithm 1 The QLN algorithm for quaternion matrix completion

Input: the incomplete matrix data $\dot{\mathbf{M}} \in \mathbb{H}^{M \times N}$, the real matrix \mathbf{W} is used to determine the position of observed and missing elements, λ, μ_{min} .

- 1: **Initial** $\dot{\mathbf{X}}_1 = \dot{\mathbf{M}}, t_1, \omega_1$.
- 2: **Repeat**
- 3: Update $\mu_{k+1}^{\dot{\mathbf{U}}} = \max \{ \|\dot{\mathbf{V}}_k\|_F^2, \mu_{min} \}$.
- 4: Update $\dot{\mathbf{U}}_{k+1}$ by (23).
- 5: Update $\mu_{k+1}^{\dot{\mathbf{V}}} = \max \{ \|\dot{\mathbf{U}}_{k+1}\|_F^2, \mu_{min} \}$.
- 6: Update $\dot{\mathbf{V}}_{k+1}$ by (34).
- 7: $k \leftarrow k + 1$.
- 8: **Until convergence**
- 9: Update $\dot{\mathbf{X}}_{opt} = \dot{\mathbf{U}}_{k+1} \dot{\mathbf{V}}_{k+1}^H$.

Output: the recovered quaternion matrix.

Definition 5. (*TQLN*): Given $\dot{\mathbf{X}} \in \mathbb{H}^{M \times N}$, the truncated logarithmic norm of the quaternion matrix with $0 \leq p \leq 1$ and $\epsilon > 0$ is defined as the sum of logarithmic function of $\min(M, N) - r$ minimum singular values:

$$\|\dot{\mathbf{X}}\|_{L,r}^p = \sum_{i=r+1}^{\min(M,N)} \log(\sigma_i^p(\dot{\mathbf{X}}) + \epsilon), \quad (35)$$

where σ_i can be obtained by the QSVD of $\dot{\mathbf{X}}$.

Since the first few largest singular values make no difference to rank, we will discard them in the TQLN and be committed to optimizing the smallest $\min(M, N) - r$ singular values to get a more accurate low rank estimation. According to the TQLN, the completion based on the low rank minimization model (12) can be formulated as follows

$$\min_{\dot{\mathbf{X}}} \|\dot{\mathbf{X}}\|_{L,r}^p, \quad \text{s.t.} \quad P_{\Omega}(\dot{\mathbf{X}} - \dot{\mathbf{M}}) = 0. \quad (36)$$

We have the following theorem based on the Von Neumann's trace inequality [30] to solve the TQLN.

Theorem 5. Given matrix $\dot{\mathbf{X}} \in \mathbb{H}^{M \times N}$, and any matrices $\dot{\mathbf{A}} \in \mathbb{H}^{r \times M}$ and $\dot{\mathbf{B}} \in \mathbb{H}^{r \times N}$ that are satisfied with $\dot{\mathbf{A}}\dot{\mathbf{A}}^H = \mathbf{I}_{r \times r}$, $\dot{\mathbf{B}}\dot{\mathbf{B}}^H = \mathbf{I}_{r \times r}$. r is any integer

($r \leq \min(M, N)$), we have

$$|tr(\dot{\mathbf{A}}\dot{\mathbf{X}}\dot{\mathbf{B}}^H)| \leq \sum_{i=1}^r \sigma_i(\dot{\mathbf{X}}). \quad (37)$$

Furthermore, $\max |tr(\dot{\mathbf{A}}\dot{\mathbf{X}}\dot{\mathbf{B}}^H)| = \sum_{i=1}^r \sigma_i(\dot{\mathbf{X}})$.

The proof of Theorem 5 can be found in the Appendix.

Then we can rewrite the model as

$$\begin{aligned} \min_{\dot{\mathbf{X}}} \lambda \|\dot{\mathbf{X}}\|_L^p - \max_{\substack{\dot{\mathbf{C}}\dot{\mathbf{C}}^H=\mathbf{I}, \dot{\mathbf{D}}\dot{\mathbf{D}}^H=\mathbf{I}}} |tr(\dot{\mathbf{C}}\dot{\mathbf{X}}\dot{\mathbf{D}}^H)|, \\ \text{s.t. } P_\Omega(\dot{\mathbf{X}} - \dot{\mathbf{M}}) = 0. \end{aligned} \quad (38)$$

This procedure is summarized in Algorithm 2.

Algorithm 2 The two-step TQLN algorithm

Input: the incomplete matrix data $\dot{\mathbf{M}} \in \mathbb{H}^{M \times N}$, the position set of observed elements Ω , and the tolerance ε_0 .

1: **Initial** $\dot{\mathbf{X}}_1 = \dot{\mathbf{M}}$.

2: **Repeat**

3: **Step 1.** Given $\dot{\mathbf{X}}_k$

$$[\dot{\mathbf{U}}_k, \dot{\Sigma}_k, \dot{\mathbf{V}}_k] = QSV D(\dot{\mathbf{X}}_k)$$

4: where $\dot{\mathbf{U}}_k = (\dot{\mathbf{u}}_1, \dots, \dot{\mathbf{u}}_m) \in \mathbb{H}^{M \times M}$,

$$\dot{\mathbf{V}}_k = (\dot{\mathbf{v}}_1, \dots, \dot{\mathbf{v}}_n) \in \mathbb{H}^{N \times N}.$$

5: Computing $\dot{\mathbf{C}}_k = (\dot{\mathbf{u}}_1, \dots, \dot{\mathbf{u}}_r)^T \in \mathbb{H}^{r \times M}$ and

$$\dot{\mathbf{D}}_k = (\dot{\mathbf{v}}_1, \dots, \dot{\mathbf{v}}_r)^T \in \mathbb{H}^{r \times N}.$$

6: **Step 2.** Solving

$$\dot{\mathbf{X}}_{k+1} = \arg \min \lambda \|\dot{\mathbf{X}}\|_L^p - tr(\dot{\mathbf{C}}_k \dot{\mathbf{X}} \dot{\mathbf{D}}_k^T)$$

7: **Until convergence** $\|\dot{\mathbf{X}}_{k+1} - \dot{\mathbf{X}}_k\|_F \leq \varepsilon_0$

Output: the recovered quaternion matrix.

In the first step, by computing QSVD of $\dot{\mathbf{X}}_k$, we can get $\dot{\mathbf{C}}_k$ and $\dot{\mathbf{D}}_k$. In step 2, we solve the model (38) by using the ADMM framework as in the complex or quaternion filed [4, 28]. We first reformulate model (38) as

$$\begin{aligned} \min_{\dot{\mathbf{X}}, \dot{\mathbf{H}}} \lambda \|\dot{\mathbf{X}}\|_L^p - |tr(\dot{\mathbf{C}}_l \dot{\mathbf{H}} \dot{\mathbf{D}}_l^H)| \\ \text{s.t. } \dot{\mathbf{X}} = \dot{\mathbf{H}} \quad P_\Omega(\dot{\mathbf{H}} - \dot{\mathbf{M}}) = 0, \end{aligned} \quad (39)$$

where $\dot{\mathbf{H}}$ is an intermediate variable. Significantly, the multiplication in the quaternion domain is not commutative, so the Lagrange function of problem (39) can be written as

$$\begin{aligned} L(\dot{\mathbf{X}}, \dot{\mathbf{H}}, \dot{\mathbf{Y}}, \beta) = & \lambda \|\dot{\mathbf{X}}\|_L^p - |\text{tr}(\dot{\mathbf{C}}_l \dot{\mathbf{H}} \dot{\mathbf{D}}_l^H)| \\ & + \frac{\beta}{2} \|\dot{\mathbf{X}} - \dot{\mathbf{H}}\|_F^2 \\ & + \Re(\text{tr}(\dot{\mathbf{Y}}^H (\dot{\mathbf{X}} - \dot{\mathbf{H}}))), \end{aligned} \quad (40)$$

where β_k is a positive penalty parameter, and $\dot{\mathbf{Y}}$ is the Lagrange multiplier.

Updating $\dot{\mathbf{X}}$: Assuming $\dot{\mathbf{X}}_{\tau+1}$ is $\tau + 1$ -th iteration result in step 2 and keeping other variables with the latest value, the optimal solution of $\dot{\mathbf{X}}_{\tau+1}$ can be obtained from the following problem

$$\begin{aligned} \dot{\mathbf{X}}_{\tau+1} = & \arg \min_{\dot{\mathbf{X}}} \lambda \|\dot{\mathbf{X}}\|_L^p + \frac{\beta_\tau}{2} \|\dot{\mathbf{X}} - \dot{\mathbf{H}}_\tau\|_F^2 + \Re(\text{tr}(\dot{\mathbf{Y}}_\tau^H (\dot{\mathbf{X}} - \dot{\mathbf{H}}_\tau))) \\ = & \arg \min_{\dot{\mathbf{X}}} \lambda \|\dot{\mathbf{X}}\|_L^p + \frac{\beta_\tau}{2} \|\dot{\mathbf{X}} - (\dot{\mathbf{H}}_\tau - \frac{1}{\beta_\tau} \dot{\mathbf{Y}}_\tau)\|_F^2 \end{aligned} \quad (41)$$

Utilizing the QLSVT, when let $p = 1$, $\dot{\mathbf{A}} = \dot{\mathbf{H}}_\tau - \frac{1}{\beta_\tau} \dot{\mathbf{Y}}_\tau$, we can get

$$\dot{\mathbf{X}}_{\tau+1} = \dot{\mathbf{U}}_{\dot{\mathbf{A}}} \mathcal{L}_{\frac{\lambda}{\beta_\tau}, \epsilon}(\Lambda_{\dot{\mathbf{A}}}) \dot{\mathbf{V}}_{\dot{\mathbf{A}}}^H \quad (42)$$

Updating $\dot{\mathbf{H}}$: Fixing $\dot{\mathbf{X}}_{\tau+1}$ and $\dot{\mathbf{Y}}_\tau$, the optimal solution of $\dot{\mathbf{H}}_{\tau+1}$ can be obtained from the following problem

$$\begin{aligned} \dot{\mathbf{H}}_{\tau+1} = & \arg \min_{\dot{\mathbf{H}}} -|\text{tr}(\dot{\mathbf{C}}_l \dot{\mathbf{H}} \dot{\mathbf{D}}_l^H)| + \frac{\beta_\tau}{2} \|\dot{\mathbf{X}}_{\tau+1} - \dot{\mathbf{H}}\|_F^2 + \Re(\text{tr}(\dot{\mathbf{Y}}_\tau^H (\dot{\mathbf{X}}_{\tau+1} - \dot{\mathbf{H}}))) \\ = & \arg \min_{\dot{\mathbf{H}}} \frac{\beta_\tau}{2} \|\dot{\mathbf{H}} - (\dot{\mathbf{X}}_{\tau+1} + \frac{1}{\beta_\tau} (\dot{\mathbf{C}}_l^H \dot{\mathbf{D}}_l + \dot{\mathbf{Y}}_\tau))\|_F^2. \end{aligned} \quad (43)$$

The closed solution of $\dot{\mathbf{H}}_{\tau+1}$ can be attained by

$$\dot{\mathbf{H}}_{\tau+1} = \dot{\mathbf{X}}_{\tau+1} + \frac{1}{\beta_\tau} (\dot{\mathbf{C}}_l^H \dot{\mathbf{D}}_l + \dot{\mathbf{Y}}_\tau). \quad (44)$$

Then, we let the values of all observed elements be constant in each iteration and reach

$$\dot{\mathbf{H}}_{\tau+1} = P_{\Omega^C}(\dot{\mathbf{H}}_{\tau+1}) + P_{\Omega}(\dot{\mathbf{M}}). \quad (45)$$

Updating $\dot{\mathbf{Y}}_{\tau+1}$: Fixing $\dot{\mathbf{X}}_{\tau+1}$ and $\dot{\mathbf{H}}_{\tau+1}$, the optimal solution of $\dot{\mathbf{Y}}_{\tau+1}$ can be obtained from the following problem:

$$\dot{\mathbf{Y}}_{\tau+1} = \dot{\mathbf{Y}}_{\tau} + \beta_{\tau}(\dot{\mathbf{X}}_{\tau+1} - \dot{\mathbf{H}}_{\tau+1}). \quad (46)$$

Updating the penalty parameter $\beta_{\tau+1}$:

$$\beta_{\tau+1} = \rho\beta_{\tau}. \quad (47)$$

The whole procedure in step 2 is summarized in Algorithm 3.

Algorithm 3 The optimization of TQLN using ADMM in step 2

Input: $\dot{\mathbf{M}}, \dot{\Omega}, \dot{\mathbf{C}}_l, \dot{\mathbf{D}}_l$, and the tolerance $\varepsilon, \lambda, \rho, \beta_{max}$.

1: **Initial** $\dot{\mathbf{X}}_1 = \dot{\mathbf{M}}, \dot{\mathbf{H}}_1 = \dot{\mathbf{X}}_1, \dot{\mathbf{Y}}_1 = \dot{\mathbf{X}}_1$, and β_1 .

2: **Repeat**

3: Update $\dot{\mathbf{X}}_{\tau+1} = \dot{\mathbf{U}}_{\dot{\mathbf{A}}} \mathcal{L}_{\frac{\lambda}{\beta_{\tau}}, \epsilon}(\dot{\Lambda}_{\dot{\mathbf{A}}}) \dot{\mathbf{V}}_{\dot{\mathbf{A}}}^H$.

4: Update $\dot{\mathbf{H}}_{\tau+1} = \dot{\mathbf{X}}_{\tau+1} + \frac{1}{\beta_{\tau}}(\dot{\mathbf{C}}_l^H \dot{\mathbf{D}}_l + \dot{\mathbf{Y}}_{\tau})$

5: Update $\dot{\mathbf{Y}}_{\tau+1} = \dot{\mathbf{Y}}_{\tau} + \beta_{\tau}(\dot{\mathbf{X}}_{\tau+1} - \dot{\mathbf{H}}_{\tau+1})$.

6: Update $\beta_{\tau+1} = \min(\rho\beta_{\tau}, \beta_{max})$

7: $\tau \leftarrow \tau + 1$

8: **Until convergence** $\|\dot{\mathbf{X}}_{\tau+1} - \dot{\mathbf{X}}_{\tau}\|_F \leq \varepsilon$

Output: $\dot{\mathbf{X}}_{\tau+1}, \dot{\mathbf{H}}_{\tau+1}, \dot{\mathbf{Y}}_{\tau+1}$.

4. Experimental results

In this section, we verify the performance of the proposed TQNF and TQLNA methods. We compare relevant and state-of-art algorithms:

1. **WNNM** [7]: the weighted nuclear norm of the real matrix is used to depict low rank.
2. **TNNR** [1]: the truncated nuclear norm of the real matrix is used to avoid the largest several singular values being punished much.
3. **D-N** [2]: the real bilinear factor matrices are proposed to depict low rank based on nuclear norm.
4. **F-N** [2]: the real bilinear factor matrices are proposed to depict low rank based on Frobenius norm.



Figure 2: The 8 color images (from left to right, Image(1) $300 \times 300 \times 3$, Image(2) $300 \times 300 \times 3$, Image(3) $300 \times 300 \times 3$, Image(4) $300 \times 300 \times 3$, Image(5) $300 \times 300 \times 3$, Image(6) $300 \times 300 \times 3$, Image(7) $300 \times 300 \times 3$, and Image(8) $300 \times 300 \times 3$).

5. **LRMF** [24]: the real factor matrices are proposed to depict low rank based on Logarithmic norm.
6. **LRQA-2** [3]: the Laplace function is used to replace QNN to depict the low rank of quaternion matrix.
7. **Q-DNN** [4]: bilinear factor quaternion matrices factorization is designed based on QNN.
8. **Q-FNN** [4]: bilinear factor quaternion matrices factorization is designed based on quaternion Frobenius norm.

All the experiments are operated in Matlab R2019a, on a PC with a 3.00GHz CPU and RAM of 8GB.

Parameters setting: For QLNF, we let $t_1 = 1$, $\omega_0 = 0$, $\lambda = 1.25e - 5$, and $\mu_{\min} = 0.005$. The stopping criterion is defined as $means(\|\dot{\mathbf{U}}_{k+1} - \dot{\mathbf{U}}_k\|_F / \|\dot{\mathbf{U}}_k\|_F, \|\dot{\mathbf{V}}_{k+1} - \dot{\mathbf{V}}_k\|_F / \|\dot{\mathbf{V}}_k\|_F) \leq \epsilon_0$, where $\epsilon_0 = 0.001$. The appropriate d is chosen from $\{6, 8, 10, 20\}$. For TQLNA, due to the lack of prior knowledge of the number of truncated singular values, letting $r = 1$ to report the experimental results, the better results can be achieved with appropriate adjustments of r . We let $\rho = 1.5$, $\beta_{max} = 10^7$, and $\beta_0 = 0.003$. The stopping criterion is $\|\dot{\mathbf{X}}_{k+1} - \dot{\mathbf{X}}_k\|_F / \|\dot{\mathbf{M}}\|_F \leq \epsilon_0$, where $\epsilon_0 = 0.001$. The parameters of these compared methods are set as the experimental settings reported in their papers individually. Eight frequently used color images are selected as test samples, which are shown in Figure 2.

Performance index setting: The peak signal to noise rate (PSNR) and the structural similarity index (SSIM) are adopted to compare the quality of reconstruction results. The best results are **bolded** in experiments. For quaternion-based approaches, we load the test image as a whole quaternion matrix. Matrix-based approaches are performed on each channel of the test image respectively. The smaller value of Sampling Rate (SR) represents the higher degree of missing.

Table 1 and Table 2 display the results of recovering these 8 images. The PSNR, SSIM, and average CPU time (seconds) of all testing images

reconstructed by 10 utilized recovering methods for different SRs (10%, 15%, 25%, 35%, 45%, and 50%, respectively). Figure 3 displays the corresponding visual comparisons of SR = 15% between the two designed methods and other methods of comparison on the above eight tested color images.

Figure 4 compares the visual results among all competing inpainting methods on recovering image(8) with SR = 20%. The corresponding PSNR and SSIM are given in Table 3. By comparing PSNR values, we also test the robustness of TQLNA with different truncated number $r \in [1, 20]$ when SR = 40% in Figure 5.

In addition to the above eight images, we randomly select 60 color images from Berkeley Segmentation Dataset (BSD)¹ to fully explain the effectiveness of the proposed algorithms. In Figure 6, we map out the PSNR and SSIM values on the 60 color images with SR = 20%. The average values are reported in Table 4. Similarly, in Figure 7, we map out the PSNR and SSIM values on the 60 color images with SR = 40%. The average values are reported in Table 5. All the straight lines represent the average results obtained by ten methods.

From the above experimental results, we can draw the following summaries.

- When testing the eight images, we set SR= 10% as an extreme case. In these experiments, we find that our methods are able to get higher PSNR and SSIM values in most cases (Six-eighths) without changing the truncated number r of TQLNA method. For QLNF method, it also attains better parameter results when the missing rate is high. On the contrary, when SR= 50%, the TQLNA method is the most effective way to restore images from the respect of PSNR and SSIM values. In Figure 4, it is observed that TQLNA recovery more details of the zoomed-in section, and Table 3 further confirms this conclusion. This is mainly as a result of the superiority from the quaternion representation of color pixel values.
- When using the BSD datasets, we set SR= 20% and SR= 40% and draw the PSNR, SSIM values and average values of each picture. The TQLNA method is able to achieve better results in almost all cases, but the effectiveness of QLNF method would be slightly reduced when the

¹Available: <https://www2.eecs.berkeley.edu/Research/Projects/CS/vision/bsds/>

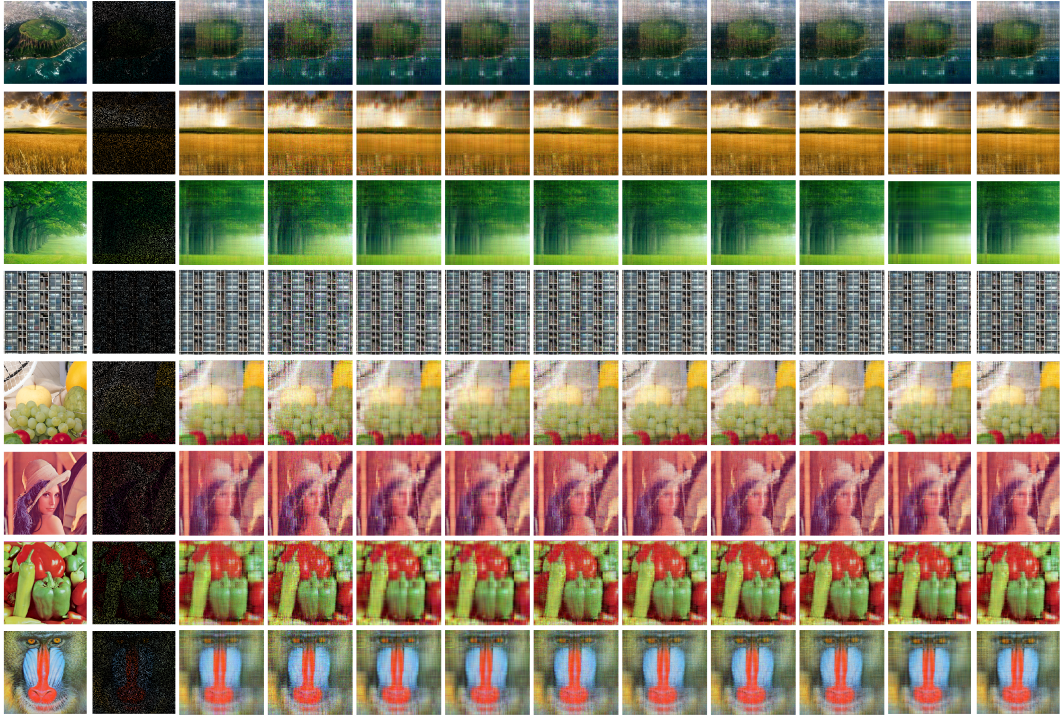


Figure 3: The first column is the original image and the second column is the observed image (SR=15%). The 3-th to 12-th are the completion results of TNNR, WNNR, D-N, F-N, LRMF, LRQA-2, Q-DNN, Q-FNN, QLNLF, and TQLNA, respectively. The corresponding parameters are summarized in Table 1 and Table 2.

degree of absence is lower. Besides, the TNNR method can also reach superior results. Profiting from this truncated skill, our quaternion-based method is optimized.

- For the time consumption, the matrix-based factorization methods like D-N, F-N are much more time-saving than others. This is due to only two smaller factor matrices need to be handled. Although our method is a bit time-consuming, it still reduces the time cost in the quaternion domain, especially for TQLNA method.

5. Conclusion

In this paper, we propose two models for low-rank quaternion matrix completion by (1) combining low-rank quaternion matrix factorization and

Image	SR Method	10%		15%		25%		35%		45%		50%		Aver. Time
		PSNR	SSIM	PSNR	SSIM	PSNR	SSIM	PSNR	SSIM	PSNR	SSIM	PSNR	SSIM	
Image(1)	TNNR	18.316	0.408	19.469	0.512	21.265	0.628	22.674	0.713	24.135	0.787	24.949	0.819	98.122
	WNNR	14.676	0.283	16.538	0.332	18.424	0.451	20.110	0.563	21.584	0.656	22.402	0.701	37.956
	D-N	17.929	0.3694	18.831	0.429	20.139	0.512	20.697	0.545	20.924	0.559	21.050	0.567	1.889
	F-N	18.289	0.385	19.063	0.438	20.225	0.514	20.716	0.545	20.954	0.559	21.054	0.568	1.244
	LRMF	17.830	0.376	18.444	0.427	18.790	0.460	20.643	0.572	22.200	0.652	22.697	0.678	1.451
	LRQA-2	18.788	0.448	19.645	0.514	21.163	0.615	22.598	0.703	24.052	0.778	24.876	0.811	81.105
	Q-DNN	18.529	0.436	19.334	0.486	20.773	0.583	22.091	0.664	23.261	0.724	23.900	0.753	28.717
	Q-FNN	18.779	0.448	19.546	0.496	20.808	0.576	22.130	0.654	23.385	0.727	24.515	0.786	30.628
	QLNF	18.668	0.427	19.443	0.482	20.699	0.560	21.525	0.606	22.461	0.662	22.955	0.689	39.814
SQLNA	18.817	0.453	19.831	0.529	21.357	0.630	22.766	0.713	24.260	0.786	25.053	0.817	28.507	
Image(2)	TNNR	20.630	0.813	21.951	0.856	23.629	0.898	25.226	0.929	26.745	0.950	27.489	0.959	24.005
	WNNR	14.087	0.572	19.136	0.749	21.282	0.832	23.042	0.886	24.543	0.920	25.269	0.934	35.459
	D-N	19.985	0.793	21.140	0.830	22.260	0.864	22.755	0.877	22.989	0.884	23.068	0.886	1.673
	F-N	20.251	0.807	21.220	0.834	22.381	0.866	22.772	0.877	22.991	0.883	23.071	0.886	1.106
	LRMF	20.111	0.794	21.996	0.854	22.432	0.872	23.602	0.900	24.611	0.920	25.101	0.927	1.324
	LRQA-2	20.863	0.821	21.852	0.851	23.564	0.894	25.072	0.924	26.505	0.945	27.253	0.954	76.154
	Q-DNN	20.606	0.816	21.996	0.856	23.385	0.892	24.935	0.923	25.980	0.938	26.584	0.945	27.809
	Q-FNN	20.775	0.819	21.996	0.856	23.466	0.894	24.745	0.919	25.715	0.935	26.468	0.945	29.920
	QLNF	20.732	0.819	21.666	0.846	22.805	0.879	23.363	0.892	24.114	0.909	24.302	0.913	40.087
SQLNA	20.955	0.822	22.079	0.857	23.734	0.899	25.390	0.930	26.881	0.951	27.680	0.961	23.756	
Image(3)	TNNR	21.291	0.807	22.957	0.856	24.380	0.893	25.794	0.920	27.183	0.941	27.867	0.949	108.649
	WNNR	16.636	0.619	19.984	0.737	21.707	0.808	23.351	0.862	24.794	0.897	25.548	0.912	37.360
	D-N	21.358	0.808	22.337	0.838	23.312	0.867	23.775	0.879	24.021	0.885	24.090	0.887	1.799
	F-N	21.676	0.820	22.590	0.846	23.437	0.870	23.819	0.880	24.011	0.885	24.088	0.887	1.144
	LRMF	21.321	0.804	22.291	0.830	23.050	0.854	24.288	0.885	25.405	0.908	25.803	0.915	1.369
	LRQA-2	22.155	0.836	23.053	0.859	24.235	0.890	25.643	0.918	27.028	0.938	27.698	0.947	80.198
	Q-DNN	21.798	0.827	22.818	0.850	24.029	0.882	25.355	0.910	26.376	0.927	26.900	0.934	28.708
	Q-FNN	22.154	0.837	23.108	0.860	24.194	0.886	25.236	0.907	26.363	0.926	26.919	0.934	30.493
	QLNF	21.848	0.837	22.683	0.856	23.397	0.872	24.116	0.887	24.452	0.893	24.558	0.896	32.660
SQLNA	22.318	0.845	23.286	0.868	24.578	0.898	25.943	0.923	27.385	0.943	28.076	0.951	18.037	
Image(4)	TNNR	17.356	0.722	19.558	0.814	22.664	0.894	25.037	0.934	27.159	0.958	28.293	0.968	43.968
	WNNR	11.990	0.392	17.031	0.683	21.572	0.856	24.269	0.917	26.275	0.945	27.231	0.956	35.826
	D-N	17.495	0.712	19.399	0.799	20.661	0.844	21.055	0.858	21.323	0.866	21.404	0.868	1.928
	F-N	17.685	0.717	19.428	0.801	20.588	0.840	21.062	0.858	21.312	0.865	21.378	0.865	1.222
	LRMF	17.023	0.686	19.151	0.782	22.464	0.881	24.763	0.925	26.008	0.942	26.358	0.947	1.269
	LRQA-2	17.962	0.743	20.135	0.825	23.281	0.903	25.521	0.939	27.578	0.960	28.577	0.968	77.018
	Q-DNN	17.894	0.742	19.913	0.813	23.290	0.901	25.697	0.940	27.690	0.960	28.534	0.967	28.371
	Q-FNN	17.767	0.733	19.922	0.816	23.508	0.907	25.616	0.939	26.849	0.953	27.627	0.960	30.187
	QLNF	17.881	0.739	19.764	0.816	22.461	0.887	23.831	0.913	24.511	0.923	24.995	0.931	38.249
SQLNA	18.023	0.744	20.100	0.825	23.380	0.904	25.843	0.942	28.165	0.965	29.210	0.973	36.940	

Table 1: THE PSNR and SSIM obtained by different completion algorithms for 8 color images (image(1)-image(4))

Image	SR	10%		15%		25%		35%		45%		50%		Aver. Time
		Method	PSNR	SSIM	PSNR	SSIM	PSNR	SSIM	PSNR	SSIM	PSNR	SSIM	PSNR	
Image(5)	TNNR	16.944	0.625	19.200	0.700	21.326	0.781	23.148	0.837	24.664	0.874	25.308	0.891	67.839
	WNNR	11.828	0.370	16.773	0.556	19.286	0.670	21.185	0.747	22.735	0.797	23.327	0.814	34.571
	D-N	17.532	0.614	18.622	0.674	19.709	0.730	20.294	0.759	20.559	0.771	20.619	0.775	1.778
	F-N	17.751	0.630	18.760	0.687	19.782	0.737	20.312	0.761	20.599	0.774	20.604	0.776	1.181
	LRMF	17.166	0.600	18.234	0.641	19.731	0.701	21.722	0.773	23.002	0.811	23.402	0.825	1.358
	LRQA-2	18.264	0.663	19.598	0.715	21.459	0.781	23.209	0.833	24.609	0.867	25.277	0.882	69.690
	Q-DNN	17.940	0.635	19.240	0.688	21.279	0.765	23.005	0.818	24.220	0.847	24.730	0.858	28.348
	Q-FNN	18.484	0.672	19.649	0.716	21.495	0.777	23.031	0.821	24.454	0.855	25.016	0.869	30.952
	QLNF	18.115	0.649	19.212	0.697	21.063	0.768	22.258	0.805	23.090	0.827	23.247	0.835	43.310
	TQLNA	18.411	0.668	19.767	0.723	21.788	0.797	23.670	0.850	25.174	0.883	25.822	0.898	33.542
Image(6)	TNNR	18.229	0.789	20.126	0.849	22.258	0.897	24.142	0.928	25.989	0.950	26.842	0.959	21.895
	WNNR	12.955	0.542	17.738	0.735	20.348	0.829	22.417	0.886	24.082	0.918	24.955	0.932	38.762
	D-N	18.025	0.778	19.787	0.840	20.950	0.874	21.362	0.887	21.599	0.893	21.691	0.897	1.783
	F-N	18.203	0.794	19.953	0.848	20.979	0.878	21.369	0.889	21.613	0.895	21.681	0.896	1.117
	LRMF	17.583	0.757	19.370	0.813	20.830	0.851	22.952	0.901	24.327	0.926	24.796	0.933	1.302
	LRQA-2	18.579	0.804	20.394	0.852	22.502	0.898	24.249	0.927	25.990	0.948	26.861	0.957	74.180
	Q-DNN	18.508	0.795	20.198	0.842	22.380	0.892	24.180	0.924	25.579	0.942	26.195	0.949	28.342
	Q-FNN	18.528	0.801	20.331	0.849	22.502	0.895	24.011	0.921	25.496	0.941	26.206	0.949	30.626
	QLNF	18.444	0.801	20.227	0.850	22.053	0.891	23.063	0.910	23.834	0.922	24.369	0.930	39.760
	TQLNA	18.439	0.796	20.507	0.857	22.767	0.904	24.625	0.933	26.488	0.954	27.309	0.961	29.378
Image(7)	TNNR	16.956	0.750	18.966	0.824	21.550	0.889	23.858	0.929	25.779	0.952	26.804	0.962	45.206
	WNNR	12.796	0.507	16.699	0.713	19.888	0.834	22.302	0.896	24.227	0.931	25.011	0.941	36.000
	D-N	17.164	0.752	18.564	0.810	19.422	0.840	19.874	0.855	20.060	0.861	20.152	0.864	1.980
	F-N	17.217	0.756	18.602	0.813	19.456	0.842	19.830	0.854	20.059	0.861	20.137	0.863	1.213
	LRMF	16.363	0.716	18.153	0.786	20.773	0.864	23.113	0.914	24.342	0.933	24.762	0.939	1.269
	LRQA-2	17.419	0.769	19.568	0.838	22.140	0.898	24.402	0.935	26.301	0.957	27.298	0.965	77.539
	Q-DNN	17.187	0.752	19.301	0.824	21.992	0.892	24.289	0.932	25.852	0.952	26.517	0.958	28.411
	Q-FNN	17.505	0.774	19.788	0.844	22.474	0.904	24.285	0.933	25.898	0.953	26.816	0.961	31.637
	QLNF	17.237	0.763	19.483	0.835	21.682	0.889	23.331	0.920	24.168	0.933	24.063	0.931	36.881
	TQLNA	17.549	0.774	19.826	0.848	22.528	0.908	25.000	0.944	26.877	0.963	27.926	0.971	31.453
Image(8)	TNNR	18.923	0.548	20.234	0.612	22.100	0.713	23.682	0.786	25.318	0.848	26.192	0.873	20.206
	WNNR	13.683	0.305	17.220	0.460	19.279	0.577	21.084	0.680	22.934	0.767	23.726	0.798	35.519
	D-N	18.405	0.515	19.859	0.574	21.084	0.630	21.437	0.646	21.663	0.657	21.716	0.658	1.696
	F-N	18.767	0.527	19.999	0.581	21.118	0.631	21.454	0.645	21.664	0.656	21.712	0.658	1.088
	LRMF	18.278	0.501	19.203	0.552	20.115	0.614	21.893	0.698	23.342	0.752	23.759	0.766	1.331
	LRQA-2	19.211	0.559	20.341	0.611	22.036	0.706	23.615	0.780	25.271	0.842	26.086	0.865	73.468
	Q-DNN	18.895	0.535	19.939	0.589	21.678	0.686	23.037	0.750	24.467	0.807	24.992	0.824	28.448
	Q-FNN	19.176	0.550	20.290	0.603	21.944	0.686	23.247	0.748	24.790	0.812	26.060	0.859	31.406
	QLNF	19.190	0.548	20.284	0.592	21.727	0.663	22.571	0.700	22.956	0.715	23.314	0.732	37.021
	TQLNA	19.396	0.575	20.690	0.631	22.453	0.724	23.964	0.793	25.726	0.856	26.565	0.879	26.266

Table 2: THE PSNR and SSIM obtained by different completion algorithms for 8 color images (image(5)-image(8))

Method	TNNR	WNNR	D-N	F-N	LRMF	LRQA-2	Q-DNN	Q-FNN	QLNF	TQLNA
PSNR	21.175	18.233	20.591	20.682	19.120	21.224	20.930	21.143	21.163	21.593
SSIM	0.662	0.517	0.609	0.612	0.560	0.662	0.643	0.648	0.636	0.680

Table 3: The corresponding PSNR and SSIM of Figure 4

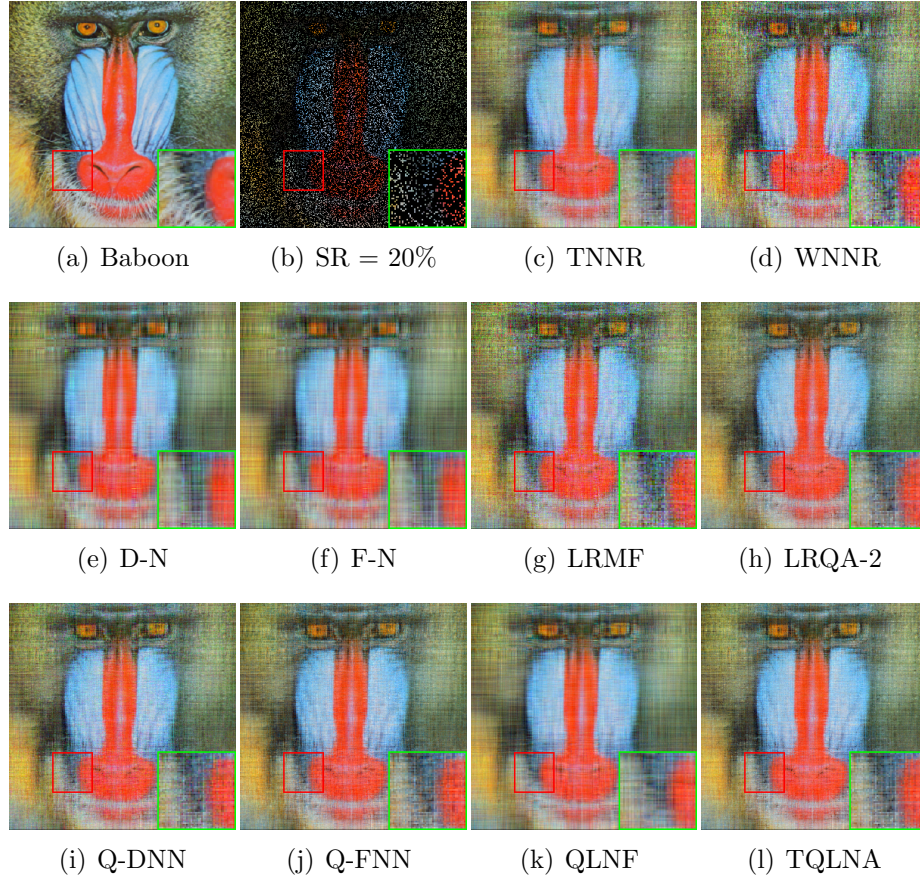


Figure 4: Color image completion results on Image (8). (a) is the original image. (b) is the observed image (SR=20%). (c)–(l) are the completion results of TNNR, WNNR, D-N, F-N, LRMF, LRQA-2, Q-DNN, Q-FNN, QLNF, and TQLNA, respectively.

Method	TNNR	WNNR	D-N	F-N	LRMF	LRQA-2	Q-DNN	Q-FNN	QLNF	TQLNA
PSNR	20.043	18.180	19.718	19.872	19.025	20.623	20.495	20.535	19.611	20.703
SSIM	0.629	0.503	0.583	0.591	0.545	0.643	0.629	0.632	0.592	0.650
Aver. Time	159.981	14.000	1.217	0.813	1.285	59.278	29.313	30.163	18.685	22.436

Table 4: The corresponding average PSNR and SSIM of Figure 6

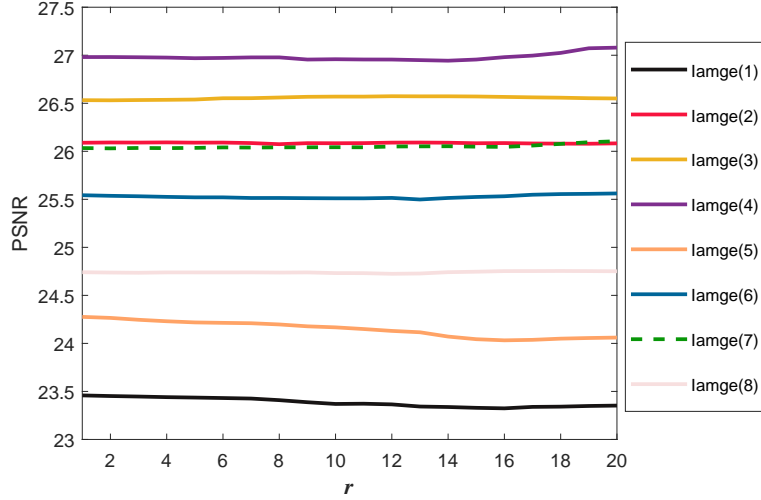


Figure 5: PSNR values of 8 images with different truncated number r when $SR=40\%$.

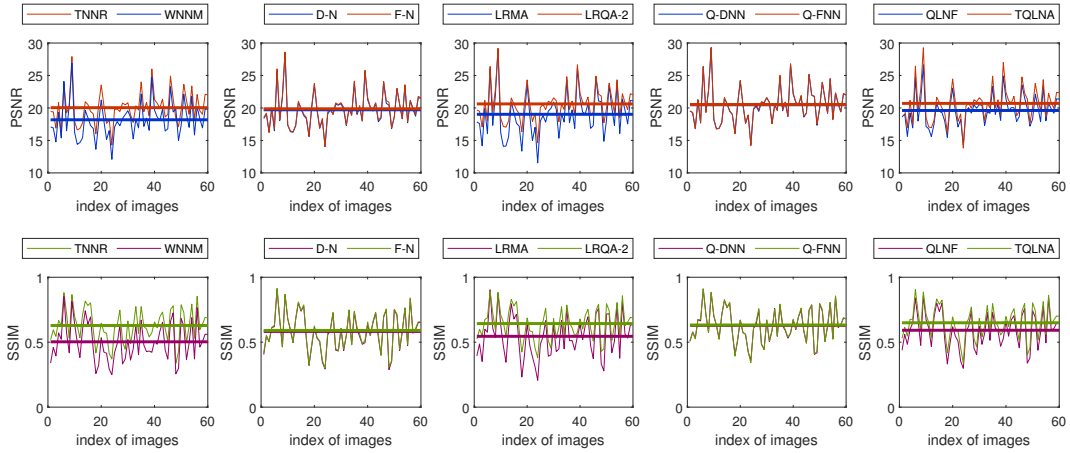


Figure 6: PSNR and SSIM values of 60 images obtained by different compared methods when let $SR=20\%$. All the straight lines are the average recovered results of these 60 images.

Method	TNNR	WNNR	D-N	F-N	LRMF	LRQA-2	Q-DNN	Q-FNN	QLNF	TQLNA
PSNR	23.775	21.606	21.245	21.264	22.093	23.667	23.388	23.273	22.099	23.959
SSIM	0.791	0.690	0.660	0.661	0.700	0.782	0.761	0.753	0.706	0.793
Aver. Time	61.451	30.491	1.405	0.981	0.936	43.223	28.437	31.051	56.257	9.789

Table 5: The corresponding average PSNR and SSIM of Figure 6

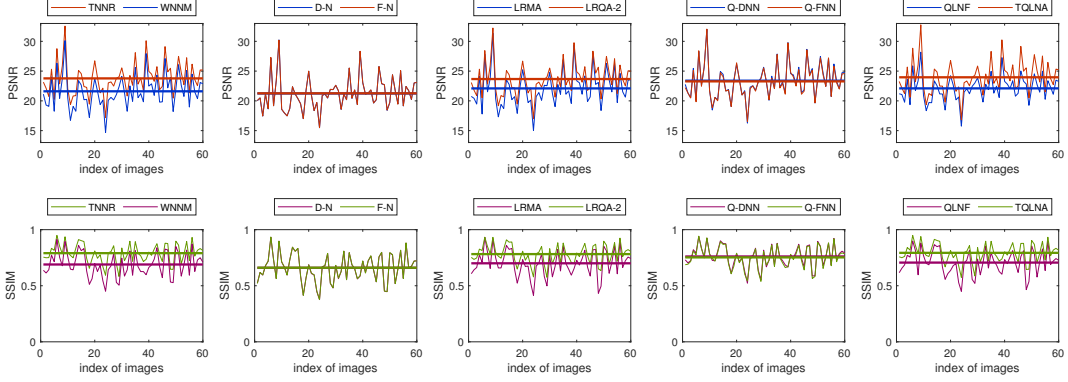


Figure 7: PSNR and SSIM values of 60 images obtained by different compared methods when let SR=40%. All the straight lines are the average recovered results of these 60 images.

logarithmic norm; (2) combining logarithmic norm to depict low rank and truncated strategy. Meanwhile, an efficient FISTA algorithm is developed to solve the proposed QLNF model, and ADMM framework is used to TQLNA model. Numerical results demonstrate that both visual and quantitative analysis can achieve superior performance by operating our methods.

In order to optimize the timewaster of QSVD, our future work is to find a more effective way to describe low-rank characteristics such as taking advantage of some convolutional neural networks (CNN), and further employ it to the quaternion domain [31].

Appendix A. The PROOF OF Theorem 3

To prove the theorem 3, we first introduce the following lemmas.

Lemma 1. *Let two quaternion matrices $\dot{\mathbf{U}} \in \mathbb{H}^{M \times r}$ and $\dot{\mathbf{V}} \in \mathbb{H}^{N \times r}$ be given with $r \leq \min M, N$, for $k = 1, \dots, r$, we have*

$$\prod_{i=1}^k \sigma_i(\dot{\mathbf{U}}\dot{\mathbf{V}}^H) \leq \prod_{i=1}^k \sigma_i(\dot{\mathbf{U}})\sigma_i(\dot{\mathbf{V}}). \quad (\text{A.1})$$

Proof:

$$\begin{aligned}
\prod_{i=1}^k \sigma_i(\dot{\mathbf{U}}\dot{\mathbf{V}}^H) &= \left(\prod_{i=1}^k \sigma_i(\dot{\mathbf{U}}\dot{\mathbf{V}}^H)_c \right)^{\frac{1}{2}} \\
&= \left(\prod_{i=1}^k \sigma_i(\dot{\mathbf{U}}_c(\dot{\mathbf{V}}^H))_c \right)^{\frac{1}{2}} \\
&\leq \left(\prod_{i=1}^k \sigma_i(\dot{\mathbf{U}}_c) \sigma_i(\dot{\mathbf{V}}^H)_c \right)^{\frac{1}{2}} \\
&= \prod_{i=1}^k \sigma_i(\dot{\mathbf{U}}) \prod_{i=1}^k \sigma_i(\dot{\mathbf{V}}),
\end{aligned} \tag{A.2}$$

where the first, second and last equalities can be proved by (5) directly (or refer to [20] for more detail), and the inequality follows from [32] (Theorem 3.3.4) \blacksquare

Based on lemma 1, we can take the logarithm to both sides of (A.1), then for $k = 1, \dots, r$

$$\sum_{i=1}^k \log(\sigma_i(\dot{\mathbf{U}}\dot{\mathbf{V}}^H)) \leq \sum_{i=1}^k \log(\sigma_i(\dot{\mathbf{U}})\sigma_i(\dot{\mathbf{V}})). \tag{A.3}$$

Lemma 2. ([32] (Corollary 3.2.11)) *Let $\mathbf{x} = [x_i]$ and $\mathbf{y} = [y_i] \in \mathbb{R}^r$ be given. $x_1 \geq \dots \geq x_r \geq 0$ and $y_1 \geq \dots \geq y_r \geq 0$. Then $\sum_{i=1}^k x_i \leq \sum_{i=1}^k y_i$ hold for $k = 1, \dots, r$ if and only if there exists a doubly stochastic matrix $\mathbf{S} \in \mathbb{R}^{r \times r}$ such that the entry-wise inequalities $\mathbf{x} \leq \mathbf{S}\mathbf{y}$ hold.*

Based on lemma 2, for inequality (A.3), when $1 \leq k \leq r$, there is a doubly stochastic matrix $\mathbf{S} \in \mathbb{R}^{n \times n}$ such that for $i = 1, \dots, r$

$$\log(\sigma_i(\dot{\mathbf{U}}\dot{\mathbf{V}}^H)) \leq \sum_{j=1}^k \mathbf{S}_{ij} \log(\sigma_j(\dot{\mathbf{U}})\sigma_j(\dot{\mathbf{V}})), \tag{A.4}$$

where \mathbf{S}_{ij} denotes the (i, j) -th element of doubly stochastic matrix \mathbf{S} ($\mathbf{S}_{ij} \geq 0$, $\sum_{i=1}^r \mathbf{S}_{ij} \geq 1$, and $\sum_{j=1}^r \mathbf{S}_{ij} \geq 1$). Then we have the following lemma, which follows from [32] (Theorem 3.3.14)

Lemma 3. Given two quaternion matrices $\dot{\mathbf{U}} \in \mathbb{H}^{M \times r}$ and $\dot{\mathbf{V}} \in \mathbb{H}^{N \times r}$ with $r \leq \min M, N$. Let $f(\cdot)$ be a real-valued function such that $\varphi(x) \equiv f(e^x)$ is convex and increasing on the range $[\min\{\sigma_r(\dot{\mathbf{U}}\dot{\mathbf{V}}^H), \sigma_r(\dot{\mathbf{U}})\sigma_r(\dot{\mathbf{V}})\}, \sigma_1(\dot{\mathbf{U}})\sigma_1(\dot{\mathbf{V}})]$, then for $k = 1, \dots, r$, we have

$$\sum_{i=1}^k f(\sigma_i(\dot{\mathbf{U}}\dot{\mathbf{V}}^H)) \leq \sum_{i=1}^k f(\sigma_i(\dot{\mathbf{U}})\sigma_i(\dot{\mathbf{V}})). \quad (\text{A.5})$$

Proof: Because $\varphi(\cdot)$ is an increasing and convex function on the given interval, for inequality (A.4) we have

$$\begin{aligned} \sum_{i=1}^k \varphi(\log(\sigma_i(\dot{\mathbf{U}}\dot{\mathbf{V}}^H))) &\leq \sum_{i=1}^k \varphi(\log(\sum_{j=1}^k \mathbf{S}_{ij} \sigma_j(\dot{\mathbf{U}})\sigma_j(\dot{\mathbf{V}}))) \\ &\leq \sum_{i=1}^k \sum_{j=1}^k \mathbf{S}_{ij} \varphi(\log(\sigma_j(\dot{\mathbf{U}})\sigma_j(\dot{\mathbf{V}}))) \\ &= \sum_{j=1}^k (\sum_{i=1}^k \mathbf{S}_{ij}) \varphi(\log(\sigma_j(\dot{\mathbf{U}})\sigma_j(\dot{\mathbf{V}}))) \\ &= \sum_{j=1}^k \varphi(\log(\sigma_j(\dot{\mathbf{U}})\sigma_j(\dot{\mathbf{V}}))), \end{aligned} \quad (\text{A.6})$$

which means that $\sum_{i=1}^k f(\sigma_i(\dot{\mathbf{U}}\dot{\mathbf{V}}^H)) \leq \sum_{i=1}^k f(\sigma_i(\dot{\mathbf{U}})\sigma_i(\dot{\mathbf{V}}))$ hold for $k = 1, \dots, r$. \blacksquare

Proof of Theorem 1:

Proof: Since the decomposition of $\dot{\mathbf{X}} = \dot{\mathbf{U}}\dot{\mathbf{V}}^H$, where $\dot{\mathbf{U}} \in \mathbb{H}^{M \times r}$

and $\dot{\mathbf{V}} \in \mathbb{H}^{N \times r}$. Denoting $K = \min(M, N, r)$, next we have

$$\begin{aligned}
2 \|\dot{\mathbf{X}}\|_L^{1/2} &= 2 \sum_{i=1}^K \log(\sigma_i^{1/2}(\dot{\mathbf{X}}) + \epsilon) = \sum_{i=1}^K 2 \log(\sigma_i^{1/2}(\dot{\mathbf{U}}\dot{\mathbf{V}}^H) + \epsilon) \\
&\leq \sum_{i=1}^K 2 \log(\sigma_i^{1/2}(\dot{\mathbf{U}})\sigma_i^{1/2}(\dot{\mathbf{V}}) + \epsilon) \\
&= \sum_{i=1}^K \log(\sigma_i(\dot{\mathbf{U}})\sigma_i(\dot{\mathbf{V}}) + 2\sqrt{\sigma_i(\dot{\mathbf{U}})\sigma_i(\dot{\mathbf{V}})}\epsilon + \epsilon^2) \\
&\leq \sum_{i=1}^K \log(\sigma_i(\dot{\mathbf{U}})\sigma_i(\dot{\mathbf{V}}) + (\sigma_i(\dot{\mathbf{U}}) + \sigma_i(\dot{\mathbf{V}}))\epsilon + \epsilon^2) \\
&= \sum_{i=1}^K \log(\sigma_i((\dot{\mathbf{U}}) + \epsilon)(\sigma_i(\dot{\mathbf{V}}) + \epsilon)) \\
&= \sum_{i=1}^K \log(\sigma_i((\dot{\mathbf{U}}) + \epsilon)) + \sum_{i=1}^K \log((\sigma_i(\dot{\mathbf{V}}) + \epsilon)) \\
&\leq \sum_{i=1}^{\min(M,r)} \log(\sigma_i((\dot{\mathbf{U}}) + \epsilon)) + \sum_{i=1}^{\min(N,r)} \log((\sigma_i(\dot{\mathbf{V}}) + \epsilon)) \\
&= \|\dot{\mathbf{U}}\|_L^1 + \|\dot{\mathbf{V}}\|_L^1,
\end{aligned} \tag{A.7}$$

where the first inequality follows from Lemma 3, as $\varphi(x) = f(e^x) = \log(e^{\frac{x}{2}} + \epsilon)$ which is an increasing and convex function on $[0, +\infty]$. Then the second inequality follows from the Young's inequality [33]. The last inequality holds due to $K = \min(M, N, r) \leq \min(M, r)$ and $K = \min(M, N, r) \leq \min(N, r)$ always hold.

Afterwards, the QSVD of $\dot{\mathbf{X}}$ is $\dot{\mathbf{X}} = \dot{\mathbf{A}}_{\dot{\mathbf{X}}}\dot{\Sigma}_{\dot{\mathbf{X}}}\dot{\mathbf{B}}_{\dot{\mathbf{X}}}^H$. Let $\dot{\mathbf{U}}_{\star} = \dot{\mathbf{A}}_{\dot{\mathbf{X}}}\dot{\Sigma}_{\dot{\mathbf{X}}}^{\frac{1}{2}}$ and $\dot{\mathbf{V}}_{\star} = \dot{\mathbf{B}}_{\dot{\mathbf{X}}}\dot{\Sigma}_{\dot{\mathbf{X}}}^{\frac{1}{2}}$. Then we can obtain $\dot{\mathbf{X}} = \dot{\mathbf{U}}_{\star}\dot{\mathbf{V}}_{\star}^H$ and $\|\dot{\mathbf{X}}\|_L^{1/2} = \frac{1}{2}(\|\dot{\mathbf{U}}_{\star}\|_L^1 + \|\dot{\mathbf{V}}_{\star}\|_L^1)$ based on the definition of the logarithmic norm with $p = 1/2$.

To sum up, we have

$$\|\dot{\mathbf{X}}\|_L^{1/2} = \min_{\substack{\dot{\mathbf{U}}, \dot{\mathbf{V}} \\ \dot{\mathbf{X}} = \dot{\mathbf{U}}\dot{\mathbf{V}}^H}} \frac{1}{2} \|\dot{\mathbf{U}}\|_L^1 + \frac{1}{2} \|\dot{\mathbf{V}}\|_L^1. \tag{A.8}$$

■

Appendix B. The PROOF OF Theorem 5

Proof: Assuming that $M \leq N$ the QSVD of the quaternion matrix $\dot{\mathbf{X}} \in \mathbb{H}^{M \times N}$ can be represented as:

$$\dot{\mathbf{X}} = \dot{\mathbf{U}} \begin{pmatrix} \boldsymbol{\Sigma}_{\tilde{r}} & \mathbf{0} \\ \mathbf{0} & \mathbf{0} \end{pmatrix} \dot{\mathbf{V}}^H = \dot{\mathbf{U}} \mathbf{D} \dot{\mathbf{V}}^H \quad (\text{B.1})$$

where $\boldsymbol{\Sigma}_r = \text{diag}(\sigma_1, \dots, \sigma_{\tilde{r}}) \in \mathbb{R}^{\tilde{r} \times \tilde{r}}$, and all singular values $\sigma_i (i = 1, \dots, r)$ are nonnegative. $\dot{\mathbf{U}} \in \mathbb{H}^{M \times M}$ and $\dot{\mathbf{V}} \in \mathbb{H}^{N \times N}$ are two unitary quaternion matrices. Then,

$$| \text{tr}(\dot{\mathbf{A}} \dot{\mathbf{X}} \dot{\mathbf{B}}^H) | = | \text{tr}(\dot{\mathbf{A}} \dot{\mathbf{U}} \mathbf{D} \dot{\mathbf{V}}^H \dot{\mathbf{B}}^H) | \quad (\text{B.2})$$

Let $\dot{\mathbf{U}}_0 = \dot{\mathbf{A}} \dot{\mathbf{U}} = (\dot{u}_{ij}) \in \mathbb{H}^{r \times M}$ and $\dot{\mathbf{V}}_0 = \dot{\mathbf{B}} \dot{\mathbf{V}} = (\dot{v}_{ij}) \in \mathbb{H}^{r \times N}$, distinctly, $\dot{\mathbf{U}}_0 \dot{\mathbf{U}}_0^H = \mathbf{I}_{r \times r}$ and $\dot{\mathbf{V}}_0 \dot{\mathbf{V}}_0^H = \mathbf{I}_{r \times r}$. Then we have

$$\begin{aligned} | \text{tr}(\dot{\mathbf{A}} \dot{\mathbf{X}} \dot{\mathbf{B}}^H) | &= | \dot{\mathbf{U}}_0 \mathbf{D} \dot{\mathbf{V}}_0^H | = \left| \sum_{i=1}^r \sum_{j=1}^M \sigma_j \dot{u}_{ij} \bar{\dot{v}}_{ij} \right| \\ &\leq \sum_{i=1}^r \sum_{j=1}^M \sigma_j | \dot{u}_{ij} \bar{\dot{v}}_{ij} | = | (1, \dots, 1)_{1 \times r} \mathbf{P}_{r \times M} (\sigma_1, \dots, \sigma_M)^T | \quad (\text{B.3}) \\ &= | (1, \dots, 1, 0, \dots, 0)_{1 \times M} \begin{pmatrix} \mathbf{P}_{r \times M} \\ \mathbf{0}_{(M-r) \times M} \end{pmatrix} (\sigma_1, \dots, \sigma_M)^T | \end{aligned}$$

where $\mathbf{P}_{r \times M} = (| \dot{u}_{ij} \bar{\dot{v}}_{ij} |)_{r \times M}$. Because

$$\sum_{i=1}^r | \dot{u}_{ij} \bar{\dot{v}}_{ij} | \leq \frac{1}{2} \left[\sum_{i=1}^r | \dot{u}_{ij} |^2 + \sum_{i=1}^r | \bar{\dot{v}}_{ij} |^2 \right] = 1 \quad (\text{B.4})$$

$$\sum_{j=1}^M | \dot{u}_{ij} \bar{\dot{v}}_{ij} | \leq \frac{1}{2} \left[\sum_{j=1}^M | \dot{u}_{ij} |^2 + \sum_{j=1}^M | \bar{\dot{v}}_{ij} |^2 \right] \leq 1 \quad (\text{B.5})$$

, $\mathbf{P}_{r \times M}$ is a doubly-substochastic matrix. According to the theories in [34]

(P 136 H.3.b) and [35] (Theorem 8.1.4 and Theorem 8.7.6), we have

$$\begin{aligned}
& | \text{tr}(\dot{\mathbf{A}}\dot{\mathbf{X}}\dot{\mathbf{B}}^H) | \\
& \leq | (1, \dots, 1, 0, \dots, 0)_{1 \times M} \begin{pmatrix} \mathbf{P}_{r \times M} \\ \mathbf{0}_{(M-r) \times M} \end{pmatrix} (\sigma_i, \dots, \sigma_M)^T | \\
& \leq | (1, \dots, 1, 0, \dots, 0)_{1 \times M} (\sigma_i, \dots, \sigma_M)^T | \\
& = \sum_{i=1}^r \sigma_i.
\end{aligned} \tag{B.6}$$

When $\dot{\mathbf{A}} = [\mathbf{I}_{r \times r}, \mathbf{0}_{(r) \times (M-r)}]\dot{\mathbf{U}}^H$ and $\dot{\mathbf{B}} = [\mathbf{I}_{r \times r}, \mathbf{0}_{(r) \times (N-r)}]\dot{\mathbf{V}}^H$, we get

$$\max | \text{tr}(\dot{\mathbf{A}}\dot{\mathbf{X}}\dot{\mathbf{B}}^H) | = \sum_{i=1}^r \sigma_i(\dot{\mathbf{X}}). \tag{B.7}$$

■

Acknowledgements

This work was supported by the Science and Technology Development Fund, Macau SAR (File no. FDCT/085/2018/A2) and University of Macau (File no. MYRG2019-00039-FST).

References

- [1] Yao Hu, Debing Zhang, Jieping Ye, Xuelong Li, and Xiaofei He. Fast and accurate matrix completion via truncated nuclear norm regularization. *IEEE Trans. Pattern Anal. Mach. Intell.*, 35(9):2117–2130, 2013.
- [2] Fanhua Shang, James Cheng, Yuanyuan Liu, Zhi-Quan Luo, and Zhouchen Lin. Bilinear factor matrix norm minimization for robust PCA: algorithms and applications. *IEEE Trans. Pattern Anal. Mach. Intell.*, 40(9):2066–2080, 2018.
- [3] Yongyong Chen, Xiaolin Xiao, and Yicong Zhou. Low-rank quaternion approximation for color image processing. *IEEE Trans. Image Process.*, 29:1426–1439, 2020.

- [4] Jifei Miao and Kit Ian Kou. Quaternion-based bilinear factor matrix norm minimization for color image inpainting. *IEEE Trans. Signal Process.*, 68:5617–5631, 2020.
- [5] Pan Zhou, Canyi Lu, Zhouchen Lin, and Chao Zhang. Tensor factorization for low-rank tensor completion. *IEEE Trans. Image Process.*, 27(3):1152–1163, 2018.
- [6] Emmanuel J. Candès and Benjamin Recht. Exact matrix completion via convex optimization. *Found. Comput. Math.*, 9(6):717–772, 2009.
- [7] Shuhang Gu, Lei Zhang, Wangmeng Zuo, and Xiangchu Feng. Weighted nuclear norm minimization with application to image denoising. In *2014 IEEE Conference on Computer Vision and Pattern Recognition, CVPR 2014, Columbus, OH, USA, June 23-28, 2014*, pages 2862–2869. IEEE Computer Society, 2014.
- [8] Yuan Xie, Shuhang Gu, Yan Liu, Wangmeng Zuo, Wensheng Zhang, and Lei Zhang. Weighted Schatten p-norm minimization for image denoising and background subtraction. *IEEE Trans. Image Process.*, 25(10):4842–4857, 2016.
- [9] Zhao Kang, Chong Peng, Jie Cheng, and Qiang Cheng. Logdet rank minimization with application to subspace clustering. *Comput. Intell. Neurosci.*, 2015:824289:1–824289:10, 2015.
- [10] Ting Xie, Shutao Li, Leyuan Fang, and Licheng Liu. Tensor completion via nonlocal low-rank regularization. *IEEE transactions on cybernetics*, 49(6):2344–2354, 2018.
- [11] Zaiwen Wen, Wotao Yin, and Yin Zhang. Solving a low-rank factorization model for matrix completion by a nonlinear successive over-relaxation algorithm. *Math. Program. Comput.*, 4(4):333–361, 2012.
- [12] Zhouchen Lin, Minming Chen, and Yi Ma. The augmented Lagrange multiplier method for exact recovery of corrupted low-rank matrices. *CoRR*, abs/1009.5055, 2010.
- [13] Jacob D. Abernethy, Francis R. Bach, Theodoros Evgeniou, and Jean-Philippe Vert. A new approach to collaborative filtering: Operator estimation with spectral regularization. *J. Mach. Learn. Res.*, 10:803–826, 2009.

- [14] Xiao-Xiao Hu and Kit Ian Kou. Phase-based edge detection algorithms. *Mathematical Methods in the Applied Sciences*, 41(11):4148–4169, 2018.
- [15] Cuiming Zou, Kit Ian Kou, Li Dong, Xianwei Zheng, and Yuan Yan Tang. From grayscale to color: Quaternion linear regression for color face recognition. *IEEE Access*, 7:154131–154140, 2019.
- [16] Yibin Yu, Yulan Zhang, and Shifang Yuan. Quaternion-based weighted nuclear norm minimization for color image denoising. *Neurocomputing*, 332:283–297, 2019.
- [17] Shan Gai, Guowei Yang, Minghua Wan, and Lei Wang. Denoising color images by reduced quaternion matrix singular value decomposition. *Multidimens. Syst. Signal Process.*, 26(1):307–320, 2015.
- [18] Sir William Rowan Hamilton LL.D. P.R.I.A. F.R.A.S. Hon. M. R. Soc. Ed. and Dub. Hon. or Corr. M. II. on quaternions; or on a new system of imaginaries in algebra. *The London, Edinburgh, and Dublin Philosophical Magazine and Journal of Science*, 25(163):10–13, 1844.
- [19] Nicolas Le Bihan and Jérôme I. Mars. Singular value decomposition of quaternion matrices: a new tool for vector-sensor signal processing. *Signal Process.*, 84(7):1177–1199, 2004.
- [20] Fuzhen Zhang. Quaternions and matrices of quaternions. *Linear algebra and its applications*, 251:21–57, 1997.
- [21] Yi Xu, Licheng Yu, Hongteng Xu, Hao Zhang, and Truong Nguyen. Vector sparse representation of color image using quaternion matrix analysis. *IEEE Trans. Image Process.*, 24(4):1315–1329, 2015.
- [22] Patrick R Girard. *Quaternions, Clifford algebras and relativistic physics*. Springer Science & Business Media, 2007.
- [23] Ricardo Silveira Cabral, Fernando De la Torre, João Paulo Costeira, and Alexandre Bernardino. Unifying nuclear norm and bilinear factorization approaches for low-rank matrix decomposition. In *IEEE International Conference on Computer Vision, ICCV 2013, Sydney, Australia, December 1-8, 2013*, pages 2488–2495. IEEE Computer Society, 2013.

- [24] Lin Chen, Xue Jiang, Xingzhao Liu, and Zhixin Zhou. Logarithmic norm regularized low-rank factorization for matrix and tensor completion. *IEEE Trans. Image Process.*, 30:3434–3449, 2021.
- [25] Maryam Fazel, Haitham Hindi, and Stephen P Boyd. Log-det heuristic for matrix rank minimization with applications to hankel and euclidean distance matrices. In *Proceedings of the 2003 American Control Conference, 2003.*, volume 3, pages 2156–2162. IEEE, 2003.
- [26] Maryam Fazel, Haitham Hindi, and Stephen P Boyd. A rank minimization heuristic with application to minimum order system approximation. In *Proceedings of the 2001 American Control Conference. (Cat. No. 01CH37148)*, volume 6, pages 4734–4739. IEEE, 2001.
- [27] Yangyang Xu and Wotao Yin. A globally convergent algorithm for non-convex optimization based on block coordinate update. *J. Sci. Comput.*, 72(2):700–734, 2017.
- [28] Lu Li, Xingyu Wang, and Guoqiang Wang. Alternating direction method of multipliers for separable convex optimization of real functions in complex variables. *Mathematical Problems in Engineering*, 2015, 2015.
- [29] Dongpo Xu and Danilo P. Mandic. The theory of quaternion matrix derivatives. *IEEE Trans. Signal Process.*, 63(6):1543–1556, 2015.
- [30] Leon Mirsky. A trace inequality of john von neumann. *Monatshefte für mathematik*, 79(4):303–306, 1975.
- [31] Xuanyu Zhu, Yi Xu, Hongteng Xu, and Changjian Chen. Quaternion convolutional neural networks. In Vittorio Ferrari, Martial Hebert, Cristian Sminchisescu, and Yair Weiss, editors, *Computer Vision - ECCV 2018 - 15th European Conference, Munich, Germany, September 8-14, 2018, Proceedings, Part VIII*, volume 11212 of *Lecture Notes in Computer Science*, pages 645–661. Springer, 2018.
- [32] Roger A. Horn and Charles R. Johnson. *Topics in Matrix Analysis*. Cambridge University Press, 1991.

- [33] William Henry Young. On classes of summable functions and their fourier series. *Proceedings of the Royal Society of London. Series A, Containing Papers of a Mathematical and Physical Character*, 87(594):225–229, 1912.
- [34] Albert W. Marshall and Ingram Olkin. *Inequalities: Theory of Majorization and Its Application*. Academic Press, 1979.
- [35] Roger A. Horn and Charles R. Johnson. *Matrix Analysis, 2nd Ed.* Cambridge University Press, 2012.